

Department of Precision and Microsystems Engineering

Measurement of cooling rate during plunge freezing of sample preparation in cryo electron microscopy

Bas Bikker

Report no : 2019.027
Coach : S. V. den Hoedt Msc. M.L., Dr. M.K. Ghatkesar
Professor : Prof. Dr. U. Staufer
Specialisation : MNE
Type of report : Thesis
Date : 29-08-2019

Master Thesis

Measurement of cooling rate during plunge
freezing of sample preparation in cryo
electron microscopy

by

B. Bikker

August 21, 2019

Student number: 4014359
Project duration: September 3, 2018 – August 29, 2019
Thesis committee: Dr. M. K. Ghatkesar, TU Delft
Prof. Dr. U. Staufer, TU Delft
S. den Hoedt MSC. M.L., Delmic B.V.

Acknowledgements

I was offered a thesis internship at Delmic BV to design, build, and carry-out experiments in the field of cryo-electron microscopy. Throughout the research, design, building, and experimenting stages of my internship at Delmic, I received support and guidance from my company supervisor, Sander den Hoedt Msc. M.L. and my TU Delft, faculty supervisor, Dr. Ghatkesar. Their interest in the development of my research and experiments, as well as my own skills and understanding of every facet of this thesis was invaluable to the progress of my work.

It is without a doubt that I not only benefited from their feedback and guidance, but from the assistance, encouragement, and feedback of many others while working on my thesis project. Therefore, I would like to express my gratitude.

To my Delmic supervisor, Sander den Hoedt Msc. M.L., thank you for the excellent feedback and interesting discussions throughout the duration of my thesis research and experimentation. Your advice frequently got me through challenging steps and over blockades in my research and experiments.

To my faculty supervisor, Dr. Ghatkesar, I'd like to firstly thank you for the time and commitment you designated to seeing me progress in my research and with my experiments. Secondly, for all your guidance and feedback throughout the challenging process of narrowing down thesis topics, developing the experiment design, the manual construction of the necessary experimental components, and the process of carrying out the experiments. And lastly, for the practical connections made between resources and people that allowed me to get my work done. Your assistance was always insightful, encouraging, and focusing.

To Dr. Jacobi, thank you for facilitating experiments at the TU Delft TNW Applied Sciences lab. Without your enthusiastic support and allowance in this matter I would not have been able to carry out my experiments.

To Daan Boltje Msc, thank you for all your assistance during the experimentation process at the TU Delft Faculty of Applied Sciences. Your assistance was instructional and allowed me to set-up and use the equipment more efficiently, which in turn gave me additional time to focus on the process of my experiments.

To my tablemates and colleagues from Delmic B.V., Shubhonil Chatterjeesc.Msc. and Xuanmin He Msc., thank you for the lively discussions, encouragement, and daily entertainment. Working with alongside you at Delmic was interesting and fun.

To my other colleagues at Delmic B.V., thank you for the professional and friendly work environment. Working with you this past year has been a unique, first experience for me. I have enjoyed getting to know each of you and look forward to working with you again in September.

To Miss Srebnicki, thank you for editing my entire thesis within a limited time-frame. Your edits and feedback helped to make this thesis read more smoothly and sound more professional.

To my parents and brother, I struggle to find words to express my gratitude for your continued love and support throughout not just my thesis project, but entire university career. I know I couldn't have come as far as I have, nor achieved all that I have, without you.

Abstract

In this thesis report, the measurements on the cooling rate of Autogrids during plunge freezing is presented. Plunge freezing is used as a sample preparation method to freeze biological samples in a vitrified thin water layer of <500 nm. Typically sample is loaded on thin (<10 nm) carbon membranes of a copper mesh grid. The vitrified biological sample is imaged using high resolution cryogenic transmission electron microscopy (Cryo-EM). The common practice of rapidly plunge freezing biological material prepares it to be placed in the vacuum chamber of the Cryo-EM by cooling it to a vitrified state (causing vitrification). In the present sample preparation methods, 90% of the biological materials used experience some form of contamination or damage during the transfer process and end up unusable.

While improvements have been made for the process to assist in the elimination of the above-mentioned issues such as the automation of sample loading into the Cryo-EM. These improvements have brought on their own set of complications. In want of a better solution for the issues surrounding the cryo-sample preparation and loading, the research and experiments of this thesis focused on the question: **is it possible for biological materials to be vitrified on an Autogrid with plunge freezing?** While there is no specific literature on EM-grids, there is a lot of research on other samples, a majority of which used a very small thermocouple in the experiments. This brought about the idea of using a very small thermocouple embedded in an EM-grid to measure the fast cooling rate during plunge freezing. It further led to the main goal of the experiments to measure the cooling rate of EM-grid and Autogrids during plunge freezing with a Vitrobot.

A small thermocouple was embedded into an EM standard-grid and Autogrid glued in place with cryo-varnish. The EM-grid was then mounted onto Vitrobot tweezers and plunged into liquid ethane (cryogen). The set-up mimics to the best of its possibilities the same conditions and procedure of the standard Cryo-EM workflow and temperature was recorded at a rate of 32000 samples per second. The cooling rate of the Autogrid is slower than that of standard grid, which implies that the Vitrobot is not capable of vitrifying biological materials on an Autogrid. Fabrication of $13\ \mu\text{m}$ diameter thermocouple was successful in creating a $40\ \mu\text{m}$ diameter bead that resulted in the cooling rate of 250×10^3 K/s being measured, this was in accordance with literature, which means that the hardware used to measure the cooling rates during the experiments was adequate. Cooling rates measured with an EM-grid were as expected.

Research and experiments showed that the Vitrobot would probably not be capable of achieving vitrification on Autogrid because the measured cooling rate was slower than that of EM-grid. Cooling rates with the Vitrobot could be improved by a faster and deeper plunger. There were significant temperature variations in the ethane bath but they were not measured immediately before plunging. This caused objective comparisons between measurements to be limited. Properly

measuring the ethane bath pre-plunging would allow for more objective comparison of the cooling rates and more reliable calculations of the heat transfer coefficient.

Contents

1	Introduction	10
1.1	Cryo-EM	11
1.2	Sample preparation	11
1.3	Vitrification	13
1.4	Freezing methods	13
1.5	Complications	14
1.5.1	Devitrification	14
1.5.2	Ice condensation	14
1.5.3	Physical damage	14
1.6	Sample preparation improvements	15
1.6.1	Research focus	15
1.7	Approach	16
2	Plunge freezing	20
3	Measurement of cooling rate during plunge freezing of sample preparation in cryo electron microscopy	22
3.1	Introduction	22
3.2	Methods	24
3.2.1	Temperature recording during plunging	24
3.2.2	Model	28
3.3	Results	29
3.3.1	Calibration	29
3.3.2	Plunge speed measurement	30
3.3.3	Cooling rate bare thermocouple	30
3.3.4	Cooling rate EM-grid and Autogrid	31
3.3.5	Convective heat transfer coefficient	36
3.3.6	COMSOL model	36
3.4	Discussion	38
3.4.1	Experiments	38
3.5	Conclusion	41
4	Reflection	43
4.1	Research focus	43
4.2	Literature research	43
4.3	Research approach	44
4.4	Thermocouple fabrication	44

4.5	Experimental research	44
4.6	Future work	45
A	Table with measurement results	46
B	Software	48
B.1	Matlab code	48
B.2	Python code	55
B.3	Arduino code	57

Chapter 1

Introduction

Developed nearly 60 years ago, Cryo-EM, or Cryogenic Electron Microscopy has been at the forefront of life sciences and pharmaceutical industries and remains one of the leading technologies in the study of macromolecular biology today. At its core, Cryo-EM uses electron imaging of cryo-immobilized biological materials under a Transmission Electron Microscope (TEM). In biology, Cryo-EM is used in a variety of different context, but typically when imaging intact and plunge-frozen biological samples.

Yet, since its development, Cryo-EM has had persistent issues surrounding plunge freezing of biological materials. Most of these issues stem from the preparation of biological materials: samples (biological materials with carrier) that are plunge frozen are incredibly delicate and prone to damages and contamination. From being handled incorrectly or indelicately and through their own rapid rise in temperature, many biological samples are not viable for the next step of the process before the transfer to the Cryo-EM is complete. With the issues involving cryo-sample preparation for the plunge freezing in mind, the main goal of this research and experiments was to explore whether it was possible to vitrify a biological sample on an Autogrid using plunge freezing. This focus question led to further research questions such as: is it possible to vitrify biological materials on an Autogrid with a Vitrobot MK IV (FEI, Eindhoven): Would a Vitrobot be fast enough? Could a Vitrobot be made faster?

Even though the Vitrobot, is the most used plunge freezing device (another popular device is the Leica EM GP2), the literature on it is more on what it is used for rather than its properties. Additionally, while there is a large amount of literary research available on the process of plunge freezing, there is very little research available specifically on the cooling rates of EM-grids or Autogrids during plunge freezing, nor any confirmed data on critical cooling rates for vitrification. Therefore, it was necessary to design an experimental situation in which the cool rates of Autogrids could be compared to EM-grids using the Vitrobot. Initial literary research suggested that the Vitrobot would not be able to cool the Autogrids fast enough for the biological materials on the grid to reach vitrification. To formally test this, it was imperative that the set-up of the experiments was constructed as close as possible to the set-up of the standard Cryo-EM workflow.

In the next chapters the reader will be introduced to the field of Cryo-EM and the complications that motivated this thesis.

1.1 Cryo-EM

Electron microscopy relies on electrons to illuminate specimens rather than photons in conventional light microscopy. The short wavelength of electrons makes it possible to generate very high resolution images up to 2.5 \AA [1]. There are two main types of Electron Microscope (EM): Transmission Electron Microscope (TEM) and Scanning Electron Microscope (SEM). In a TEM electrons that pass through the specimen are detected by a sensor behind it. For the electrons to pass through with enough energy to detect them the specimen must be thinner than 300 nm . Conventional SEM works by detecting secondary electrons that emit from the surface of the specimen. Both TEM and SEM operate under vacuum since air is not transparent to electrons. If biological specimens are to be imaged a problem arises. Biological materials (hereafter referred to as a specimen when referenced without the carrier) are mostly made up of water and would evaporate in vacuum. This is where the word 'cryo' - Ancient Greek for 'ice cold' - comes into play. Freezing water prevents it from evaporation, but the problem is that water becomes ice when frozen and the crystal structure of ice damages biological specimens. Dubouchet & McDowell (1981) [2] discovered that it is possible to vitrify water, meaning that it is solid in a glass like state without crystal structure. Vitrification has since been the preferred method in biomedical research investigating the detailed structure of tissues, cells, organelles and macro-molecular complexes.

1.2 Sample preparation

Preparing a biological sample for Cryo-EM can consist of many steps [3]. A brief example of the general workflow will now be given. The specimen of interest, for instance a protein, is first diluted to in an aqueous solution. A small volume around $3 \mu\text{L}$ of the solution is then dispensed on a sample carrier called EM-grid. This is a $25 \mu\text{m}$ thick 3 mm diameter disk within a fine mesh inside, see Fig. 1.1. The most common material used is copper. Different mesh sizes exist ranging from 100 to 600 grid holes per inch. The copper disc is usually covered with a carbon film of about 10 nm . The carbon film has many holes that vary in shape and size. Depending on the specimen a specific combinations of grid size and hole size is ideal. Handling EM-grids is done with fine tip tweezers like the Dupon #5 tweezers.

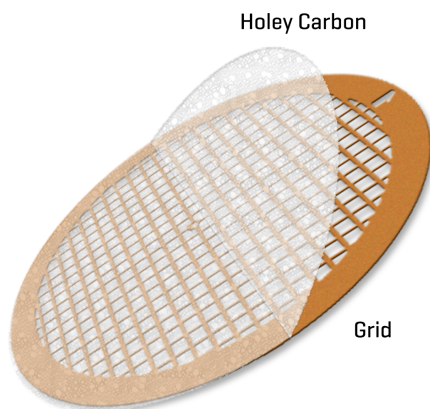


Figure 1.1: Sample carrier for Cryo-EM called EM-grid. It is a copper disk with a holey carbon film on top.

After dispensing the solution on the EM-grid, a majority of the solution has to be removed by a process called blotting to ensure a thin enough layer remains to be frozen. With blotting, excess fluid is removed by absorbing it with filter paper. Hereafter, the sample can be frozen. An in dept explanation of the freezing methods is given in a later section. From this point on the sample needs to be cooled so it is stored in a bath of liquid nitrogen (LN2) at 77 K. High-end electron microscopes have automated sample loading where the sample is transferred by a robotic arm inside the microscope. Because the EM-grid is very fragile it cannot be handled by the robotic arm. A copper supporting ring must be placed around the EM-grid to offer additional mechanical strength such that it can be handled by the robotic arm. This support is clipped around the EM-grid after it was frozen and is done while submerged in LN2. The assembly of support ring and EM-grid is called Autogrid and is shown in Fig. 1.2.

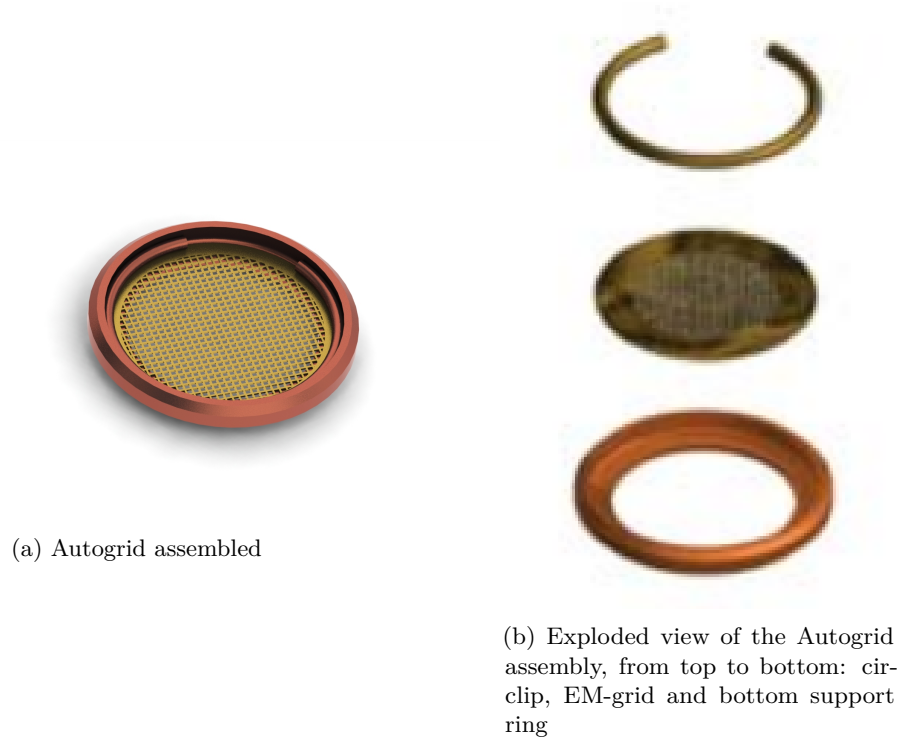


Figure 1.2: (a) Render of EM-grid and Autogrid (b) Exploded view of the Autogrid assembly

The Autogrid can then be loaded into an SEM or, if the aqueous layer is thinner than 300 nm, directly into a TEM. Some specimens like cells are thicker than 300 nm and to image them in a TEM the frozen layer has to be thinned down. This can be done by Focused Ion Beam (FIB) milling inside a SEM. During FIB milling, the sample is locally bombarded with ionized particles to mill away material leaving only a thin strip called lamella [4]. The lamella is made thin enough for electrons to pass through.

1.3 Vitrification

As mentioned before, it is important that the frozen water does not crystallize but is vitreous. Achieving this vitreous state requires very rapid cooling such that the water molecules are immobilized before nucleation of ice crystals can occur. Transformation to vitreous state happens at 140 K. A big advantage of vitrification is that it occurs within milliseconds, which means that all macro-molecular components are immobilized almost simultaneously. This makes it possible to capture their interaction. The rate at which an aqueous solution needs to be cooled for vitrification (critical cooling rate) depends, among others, on the concentration and composition of the solution and thickness of the sample. Cooling rate, CR (K s^{-1}), in this context has historically been defined as

$$CR = \frac{\Delta T}{\Delta t},$$

where $\Delta T = 273 - 173(\text{K})$ and $\Delta t(\text{s})$ is the time it takes to cool from 273 K to 173 K [5]. Vitrification of an aqueous solution of biological material has an estimated critical cooling rate of $1 \times 10^4 \text{ K s}^{-1}$ [5]. Bald (1987) [6] calculated that the critical cooling rate of a 1 μm thick sample is $3 \times 10^6 \text{ K s}^{-1}$. Increasing pressure to 2100 bar reduces the critical cooling rate of pure water to $2 \times 10^4 \text{ K s}^{-1}$ and for biological specimens to 100 K s^{-1} [7]. Attempts have been made to model vitrification [8], but they have not been confirmed with experiments. A reliable relation between cooling rate and vitrification is lacking.

1.4 Freezing methods

There are several methods to vitrify biological samples. Four popular methods will be discussed in the following sections, in order of popularity.

Plunge freezing Plunge freezing is the most popular method of vitrification. It relies on plunging the sample in a cryogenic - cold - liquid, also referred to as cryogen. It works well with EM-grids as long as the aqueous layer is less than 3 μm thick [3]. Most plunge freeze devices include automated blotting before plunging. This technique is relatively cost efficient compared to other freezing methods [9]. This method will be discussed in more detail in Chapter 3.

High pressure freezing High pressure freezing relies in the fact that at high pressure, 2100 bar, the melting point of water is lower to 253 K and the homogeneous nucleation temperature is lowered to 181 K. Therefore the critical cooling rate becomes 100 K s^{-1} . As a result, this method can be used to vitrify samples up to 200 μm . The main drawback of high-pressure freezing is the high cost of the machine[10][?].

Spray freezing During spray freezing the sample is sprayed with a cryogen, often propane. This can be done directly onto the aqueous sample or the sample is first sandwich between thin highly conductive plates and then it is sprayed on. Samples up to 13 μm can be vitrified using this technique. A newly developed spray freezing device , VitroJet (Cryosol, Maastricht), has claimed to be able of freezing Autogrids [11]. Although pricing of the Vitrojet is not yet in the public domain, it is rumored to be close to €500,000. Which is much more expensive than the cost of a plunge freezing device, around €100,000[?].

1.5 Complications

The overall yield of the current workflow for Cryo-EM is 10%, meaning that 90% of the samples that are prepared do not result in usable images. The three main causes of poor sample quality are devitrification, condensation of non-vitreous ice, and physical damage to the EM-grid. Each of these problems will be discussed in following sections. The underlying problem is the fact that most of the sample preparation involves manual transfer from one step to the next and human error is prone to happen. Because of all the manual labor it is also very time consuming. The automation of sample loading in the electron microscope increased throughput, but also introduced a step with high failure rate; during clipping of the Autogrid up to 40% of EM-grids are damaged [12].

1.5.1 Devitrification

Devitrification is the transformation of vitreous ice into crystalline ice. Crystallization damaged the structure of the sample making them unusable. Once devitrified it is not possible to recover the sample. Devitrification occurs when the sample is heated above 113 Kelvin. If the sample would be held in air at room temperature devitrification would occur in a few seconds. The common method to avoid devitrification is submersion in liquid nitrogen (LN2). LN2 has a maximum temperature of 77 Kelvin at atmospheric pressure. Within a microscope the temperature of the sample is controlled by active cooling. Risk of devitrification is high when a sample must be transferred from one LN2 bath to the other through the air. This is done by hand and must be done swiftly. Another moment in the workflow where devitrification is likely to occur is FIB milling. The ions that hit the sample transfer energy to the sample heating it up locally.

1.5.2 Ice condensation

Because the sample must be kept below 113 Kelvin, water from the air condensates on the sample and immediately freezes, but not fast enough to vitrify. This forms a layer of crystalline ice on top of the sample. The added layer of ice blurs EM images making the sample unusable. Even within the vacuum chamber of the electron microscope at 1×10^{-6} mbar there is enough water to cause problematic build-up of ice on the sample. How fast the ice condensates in each part of the workflow is unclear.

1.5.3 Physical damage

An EM-grid is very fragile. Not only is the copper body prone to bending the carbon foil on top is only 10 nm and thus extremely fragile. If the foil is touched with tweezers it is damaged, see Fig. 1.3. Consequently, picking up an EM-grid is a delicate task by itself. Having to move quickly with the sample through air to avoid devitrification adds to the complexity of the process. Most EM-grids are damaged during clipping of the Autogrid, see Fig. 1.4. Up to 40% according to a survey among users [12]. Clipping is done manually and is, to some extent, a matter of skill. A well-trained user is less likely to damage the EM-grid. It is expected that damage is done by the cir-clip slamming into the EM-grid. This could be aggravated by misalignment of the EM-grid inside the bottom support ring prior to releasing the cir-clip. Furthermore, if LN2 is trapped underneath the EM-grid sudden acceleration of the EM-grid would cause increased pressure on the foil, which could result in damage. Examination of the station the Autogrid is clipped in led to believe that there is little room for LN2 to travel through underneath the EM-grid.

1.6 Sample preparation improvements

Although Cryo-EM has been used in the field of biology since the 70's and image resolution has greatly been improved since, there is still a lot of room for improvement in the sample preparation workflow. Measuring temperature of the sample and rate of ice condensation during the whole workflow would provide knowledge on where in the workflow has the highest risks. Those parts could then be focused on first. The design of the Autogrid could be altered to reduce the change of damage during clipping. Another option would be to automate the clipping, reducing human error. Automation of the whole workflow in general would be a major improvement. Lastly, a great improvement would be to clip the Autogrid around the EM-grid at the start of the sample preparation workflow. This would not per se reduce the risk of damage by clipping but would reduce the impact of the damage done. The financial cost of an Autogrid is relatively small and since there would be no sample on the grid, nor time spent on sample preparation, simply discarding the damaged Autogrids would improve the cost effectiveness. The challenge would be to vitrify the sample within the Autogrid. Thus far, the only rapid freezing device claimed to be capable of vitrifying samples on an Autogrid is the Vitrojet (CryoSol, Maastricht) [11], although no publication were made of its capabilities at the time of writing. While a great quantity of literature was found on plunge freezing, none was specifically on Autogrids.

schematic

1.6.1 Research focus

From the above-mentioned improvements, clipping the Autogrid at the start of the workflow was deemed to be of enough interest to investigate in a thesis. And as previously mentioned the unsuccessful vitrification with the Autogrid is what prevents the implementation of this improvement. Therefore, a suitable freezing technique must be found. The first method selected to be investigated was plunge freezing because of the apparent feasibility, large amount of literature available, popularity the method already has, and availability of a plunge device for testing. The choice for this improvement was also motivated by the writer's educational background in mechanical engineering and personal fascination with plunge freezing. Plunge freezing multiple Autogrids with a standard sample following the current sample preparation workflow and imaging the frozen sample in a TEM to see if vitrification had occurred would seem like an obvious approach. If the outcome would be 'yes, vitrification has occurred,' - what is not to be expected for reason later mentioned - it would be a fast rewording approach. But, if the answer would be 'no vitrification occurred,' then the approach did not yield any new information on what could be changed to the current workflow to make vitrification possible. Also, this approach would be expensive because of the high operating cost of a TEM. Vitrification is likely to fail with an Autogrid in the current sample preparation workflow because the blotting step is not optimized for an Autogrid and to thick a liquid layer would remain to be vitrified. It would be more rewarding to measure cooling rate of an EM-grid and compare that to the cooling rate of an Autogrid. The thought is that if the Autogrid cools as fast as an EM-grid, vitrification should be possible. If the cooling rate of the Autogrid turns out to be slower, the data could still be analyzed to yield information on if and how the cooling rate could be enhanced. Hence an experimental study on cooling rate during plunge freezing for sample preparation in cryo-EM was carried out.

Based on the goal of the experiment, three main questions arose during the research and experimentation process: Is the cooling rate of an Autogrid as fast as that of EM-grid? Could the cooling rate of an Autogrid be increased with plunge freezing? How could the cooling rate of an Autogrid be increased with plunge freezing?

1.7 Approach

To be able to interpret experimental results, the thermodynamic process of plunge freezes was studied first. Based on available literature, hypotheses were drawn on events that would occur during plunge freezing. Hardware required for the experiments was purchased and fabricated and Software programs were written for data acquisition and visualization. A Finite Element Model (FEM), was generated using the prior established assumptions to predict and later verify experimental results. Plunge experiments were then carried out measuring cooling rates of EM-grids and Autogrid. The experimental results were analyzed and conclusions drawn on validity of the initial assumptions.

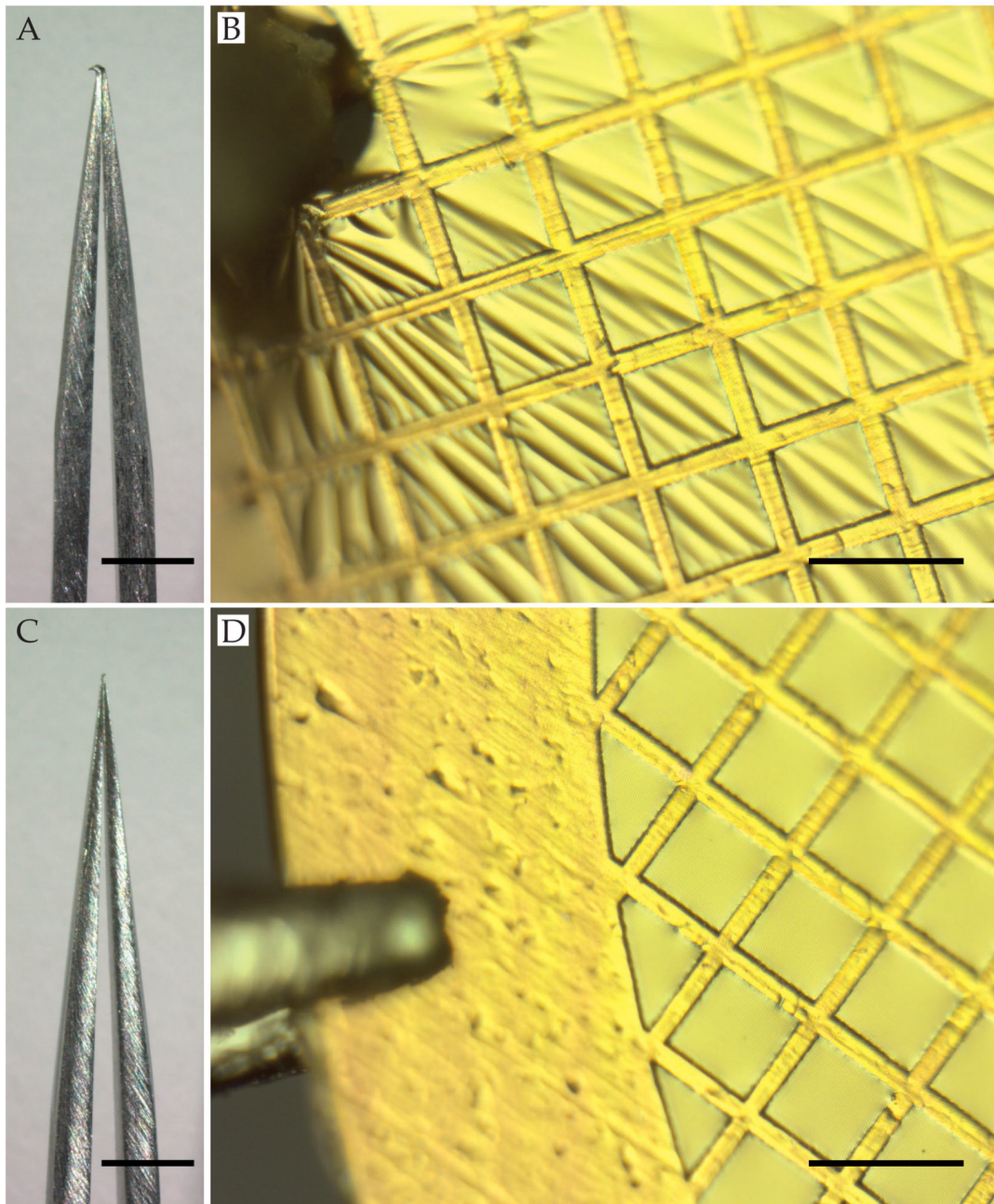


Figure 1.3: Image copied from Passmore (2016) [3]: "Tweezer damage to specimen supports. Bent tweezers (A) or improper use (B) results in damage to the specimen support. For best results, sharp, straight tweezers (C) should be used and supports should be picked up by the rim only (D). For Panels A and C, the scale bars are 1 mm. For Panels B and D, the scale bars are 100 μm ."

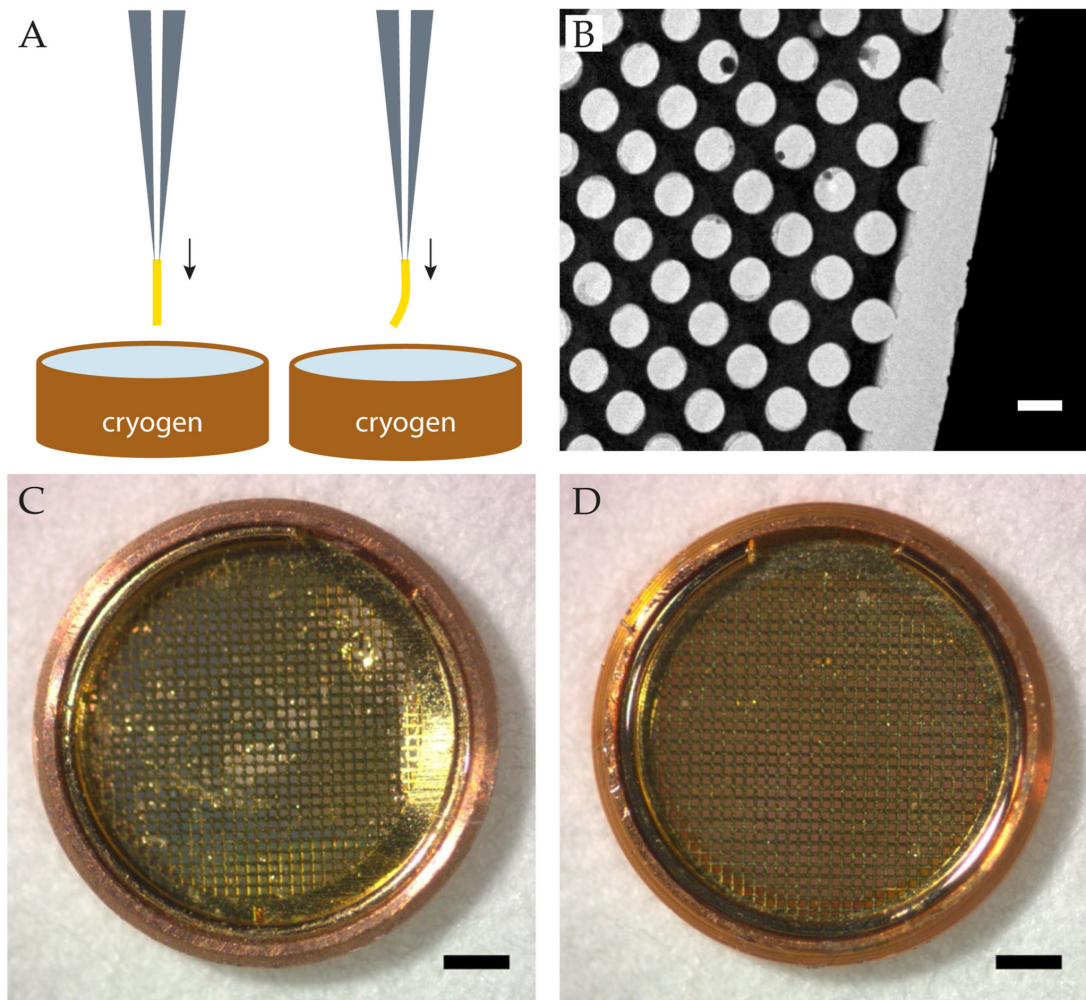


Figure 1.4: Image copied from Passmore (2016) [3]: "Vitrification and mounting of grids. (A) Supports that are bent will be damaged upon cryo plunging, resulting in broken foils. An example of a broken gold foil is shown in panel B (scale bar $2\mu\text{m}$). Supports also need to be mounted correctly in microscope cartridges. Panel C shows a support that is incorrectly mounted, and so damaged, in a Krios cartridge. The support in panel D is correctly mounted. Scale bars in panels C and D are $500\mu\text{m}$."

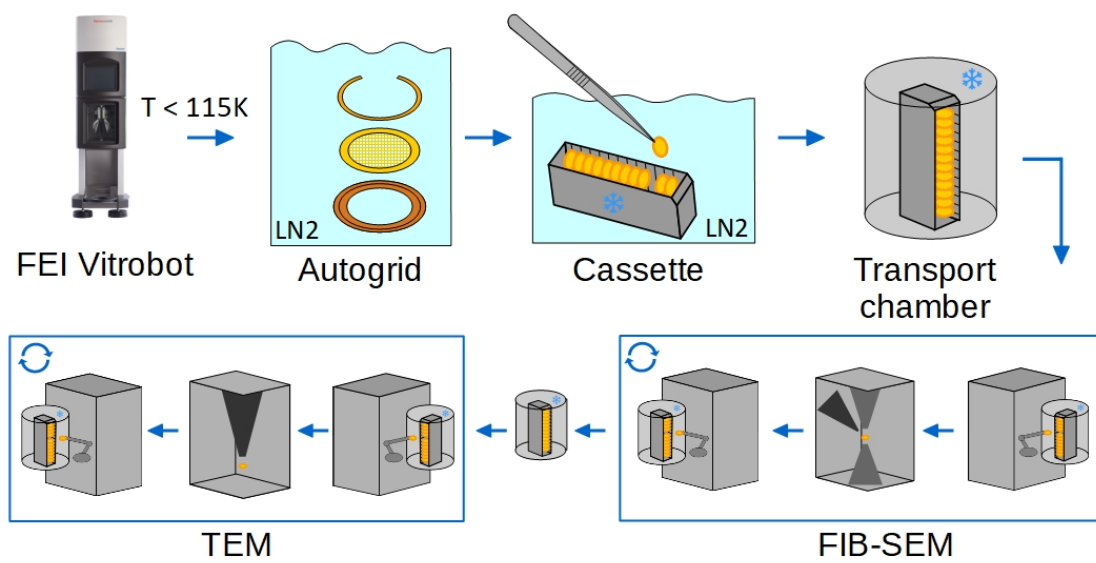


Figure 1.5: Schematic overview of the current Cryo-EM sample preparation workflow with Autogrid.

Chapter 2

Plunge freezing

The goal of plunge freezing is vitrification of an aqueous solution of biological material, further denoted as sample. To achieve this, the sample needs to cool with a certain critical cooling rate below 140 K. At atmospheric pressure, the critical cooling rate is somewhere between 10^4 K s^{-1} and $3 \times 10^6 \text{ K s}^{-1}$, dependent on the concentration and composition of the sample. With plunge freezing this is accomplished by rapid submersion in a cryogen. The first paper published on recording rapid cooling by plunging in cryogen is from Luyet & Gonzales (1951) [13]. They plunged small thermocouples in Isopentaaan. To ensure stable and reproducible velocity at immersion they build a guillotine like device where the thermocouple was attached to the falling 'blade' and the cryogen bath was placed underneath. They measured cooling rates up to $1.67 \times 10^5 \text{ K s}^{-1}$. Current plunge devices still use the guillotine principle.

However, the first successful account of vitrification by plunge freezing is from Dubochet & McDowall (1981) [2]. A typical plunge device is shown in Fig. 2.1. It consists of a frame on which an actuator is mounted. This can be pneumatic or electrically powered or rely on gravity. From the actuator extends the plunge rod with the plunge tweezers mounted to its end. The sample is hold by the tip of the tweezers. The tweezers are detachable from the plunge rod, so the tweezers can be used to pick up a sample and then be mounted on the rod. Underneath the actuator sits the LN2 bath holding the cryogen bath. The walls of the LN2 bath are made of polystyrene for good insulation, shown in purple in Fig. 2.1 and it is filled with LN2 (turquoise). The walls of the cryogen bath are typically made of copper for good conduction, shown in orange in Fig. 2.1 and it is filled with the cryogen (blue). Most cryogens have a freezing point higher than the boiling point of LN2, which means that direct cooling with LN2 would freeze the cryogen, but an insulating buffer prevents this from happening. In high end plunge devices, freezing of cryogen is prevented by heating the cryogen bath. This allows for precise temperature control of the cryogen. Modern plunge devices also include pads with filter paper for automated blotting, this is not shown in Fig. 2.1.

The next section explains which thermodynamic process are involved with plunge freezing and how the cooling is limited. As mentioned in Chapter 1.2 the EM-grid is made up from a $25 \mu\text{m}$ copper mesh grid with a diameter of 3 mm and with a 50 nm carbon foil. Typical thickness of liquid layer is 100 nm [14]. To simplify the thermodynamic model the sample will be modeled as a solid copper disk of $25 \mu\text{m}$ and a 3 mm diameter. Validity of this simplification will be given in chapter 3.3.6.

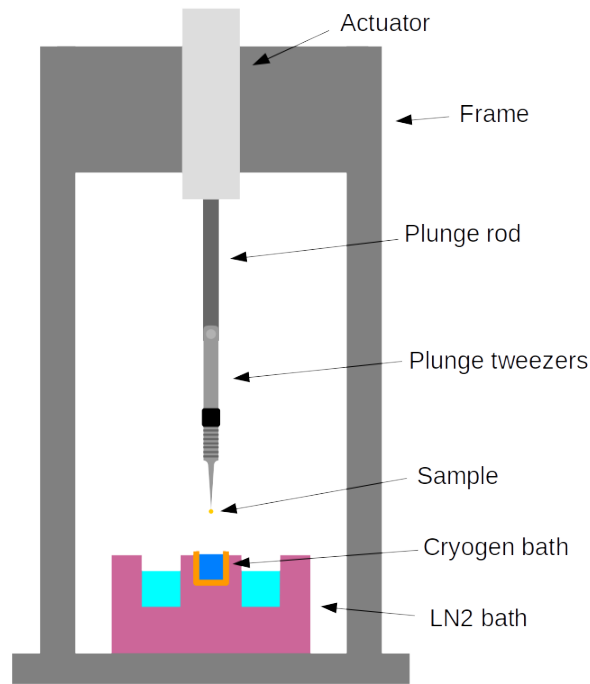


Figure 2.1: Sketch of a typical plunge device. It consists of a frame on which an actuator is mounted. From the actuator extends the plunge rod with the plunge tweezers mounted to its end. The sample is hold by the tip of the tweezers. Underneath the actuator sits the LN2 bath holding the cryogen bath.

For in depth literature on the thermodynamic processes of plunge freezing, the reader is directed to the book *Quantitative Cryofixation*, by Bald (1987) [6]. In there, the two-stage process of heat transfer from the sample to the cryogen - conduction and convection - is discussed in detail. It also informs about film boiling as a major limiting factor in fast heat transfer to the cryogen and lastly it provides the theory on how measurement data can be analyzed.

The cryogen most used is ethane, because it has high thermal conductivity and heat capacity. More important, it has a high boiling point and low melting point. This means ethane is liquid over a large temperature range and film boiling is minimized during plunging. The major drawback of ethane is that it's melting point is lower than 77 K. This means that it freezes when directly cooled with LN2. As an alternative a mixture of 35% ethane and 65% propane has been reported to perform comparable with respect to vitrification, but has as advantage that it does not freeze at 77 K[15].

Chapter 3

Measurement of cooling rate during plunge freezing of sample preparation in cryo electron microscopy

3.1 Introduction

The developed of automated sample loading for Cryo Electron Microscopy (Cryo-EM) has generated the need of a mechanically more stable sample carrier than the common EM-grid. The most used solution is the Autogrid (FEI, Eindhoven). It consists of two parts that clamp around a 3mm EM-grid, see Fig. 3.1. In the current workflow the Autogrid is clipped around the EM-grid after vitrification of the sample [4]. A survey showed that up to 40% of the samples were damaged during clipping of the Autogrid[12]. Besides possibly damaging the sample, clipping after vitrification is undesirable because handling of the vitrified sample should be minimized to avoid contamination and devitrification. Therefore, it would be advantages to clip the Autogrid around the EM-grid before vitrification. The only rapid freezing device claimed to be capable of vitrifying samples on an Autogrid is the Vitrojet (CryoSol, Maastricht) [11], although no publication were made of its capabilities at the time of writing. The technique used by the Vitrojet is spray freezing. The most used rapid freezing technique for vitrification of thin samples on an EM-grid is plunge freezing. The Vitrobot Mark IV (FEI, Eindhoven), is a commonly used device for plunge freezing. While no proof was found in literature, it is widely assumed that vitrification is not possible on an Autogrid with plunge freezing. This paper will try to give inside in the possibility of plunge freezing Autogrids.

During plunge freezing, the sample is rapidly submerged in a cryogenic fluid (cryogen), to achieve the high cooling rate required for vitrification. The theoretical minimum cooling rate required for vitrifying aqueous biological samples is reasoned to be $1 \times 10^4 \text{ K s}^{-1}$ [5], although Bald (1987) [6] calculated it to be as high as $3 \times 10^6 \text{ K s}^{-1}$. Experimental data confirming either of these numbers is lacking.

A great deal of research was done into maximizing cooling rates with plunge freezing in the 80's,

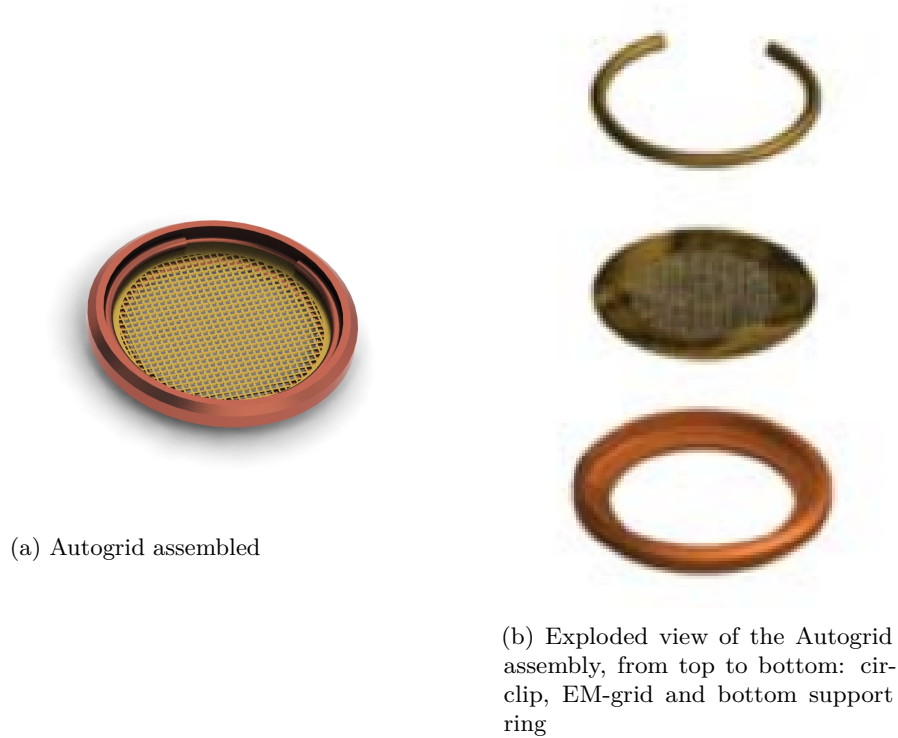


Figure 3.1: (a) Render of EM-grid and Autogrid (b) Exploded view of the Autogrid assembly

which was well documented by Ryan (1992) [16]. First account of measuring rapid cooling by plunging in cryogen is from Luyet & Gonzales (1951) [13]. They used a guillotine like device and a small thermocouple as sensor. Since then, this has been the preferred method for measuring fast cooling rates and was used in researching the best condition for plunge freezing in terms of cryogen [17][18], plunge velocity, distance [19][20], and sample support [21][22]. The successful commercial development of plunge freezing devices, like the Vitrobot, that are capable of vitrifying samples on EM-grids, as first shown by Dubochet (1981) [2], has mitigated recent research into improving plunge freezing. As a result, the cooling rate achieved by plunge freezing EM-grids have not been published. Measuring the cooling rate of an EM-grid will not only fill the knowledge gap, but also serve as a benchmark for evaluating the possibility to vitrify a sample on the Autogrid.

In order to properly interpret the experimental data, it is necessary to understand which thermodynamic process governs the cooling rate during plunge freezing. Cooling of a sample with a cryogen consists of two processes [23]. In the first process heat is conducted through the sample to the boundary of the sample. At the boundary is the interface with the cryogen. During the second process, heat is transported away from the sample through convection. The properties of the cryogen and sample determine if the cooling rate is dominated by one of the processes. The Biot number, B_i , is a dimensionless parameter that results from these properties and gives the ratio between the resistance to conductive heat transfer and the resistance to convective heat transfer. It is defined as

$$B_i \equiv (hL_c)/(k), \quad (3.1)$$

where h ($\text{W m}^{-2} \text{K}^{-1}$) is the convective heat transfer coefficient, L_c (m) is the characteristic length of the sample and k ($\text{W m}^{-1} \text{K}^{-1}$) is the thermal conductivity of the sample. If $B_i < 0.1$ the heat transfer is convection limited and if $B_i > 10$ the heat transfer is conduction limited [24]. L_c is the result of

$$\frac{V}{A_w} = L_c, \quad (3.2)$$

where V is the volume of the sample and A_w the surface area of the sample wetted by the cryogen. Historically literature has assumed that the whole surface of a sample would be wetted. However, Kasas (2003)[25] reported otherwise. High speed footage showed that when the EM-grid hits the cryogen only the circumference is being wetted. It was not clear if the wake exists after the sample was submerged.

For a bare thermocouple we can assume that all the area is wetted. The maximum heat transfer coefficient for which $B_i < 0.1$ can then be calculated with 3.1 to be $1.6 \times 10^6 \text{ W m}^{-2} \text{K}^{-1}$. If the same assumption is made for EM-grid and Autogrid then the maximum heat transfers for convection limited cooling is $1.5 \times 10^6 \text{ W m}^{-2} \text{K}^{-1}$. The assumption that all the area is wetted will be discussed later. The convective heat transfer coefficient, h , of ethane can then be calculated from the plunge cooling measurements. According to the lumped thermal capacity model this coefficient can be calculated as follows [26]:

$$h = (\rho C_p L_c)/(t) \ln(\theta_i/\theta) \quad (3.3)$$

Where ρ (kg m^{-3}) is density of the thermocouple, C_p ($\text{J kg}^{-1} \text{K}^{-1}$) is its heat capacity. L_c is the characteristic length, with is the volume to surface ratio and for a sphere this is $r/3$, where r is the radius. $\theta_i = T_i - T_\infty$, where T_i is the initial temperature and T_∞ is the temperature of the ethane. $\theta = T - T_\infty$, where T is the the temperature of the thermocouple and t is time to reach that temperature from the initial temperature. The lumped thermal capacity model is only valid in case of convection limited cooling. The cooling rates measured, discussed in chapter 3.3.4, were well below the theoretical maximum for convective cooling. With experimentally acquired cooling curves of the EM-grid and Autogrid the actual convective heat transfer can be calculated.

3.2 Methods

3.2.1 Temperature recording during plunging

EM-grids and Autogrids were plunged into liquid ethane with a Vitrobot (FEI, Eindhoven). A thermocouple glued into the centre of the grid was used to record the temperature. The thermocouples were made from $13 \mu\text{m}$ wires and had a bead of $40 \mu\text{m}$. Such a small thermocouple was required to measure the expected cooling rates in the order of $20 \times 10^3 \text{ K s}^{-1}$. According to Costello (1984) [20] and Ryan (1991) [7] the response time of such a thermocouple is 0.5 ms when plunged in ethane, measuring a cooling rate excess of $250 \times 10^3 \text{ K s}^{-1}$. Each aspect of the experiments will be discussed in the following sections.

Thermocouple fabrication and assembly

Thermocouples were made from 13 μm diameter Chromel and Alumel wire purchased from Omega Engineering Inc., Norwalk, USA. The wires were arc welded in a similar manner to the method described by Gelb (1964) [27], forming a bead of approximately 40 μm . After welding the bead the thermocouple leads were cut from the spools at a length of 10 cm. Securing a thermocouple to a EM-grid was a challenge. Good thermal contact between EM-grid and thermocouple is crucial for measuring the cooling rate of the EM-grid. The glue used to secure the thermocouple to the EM-grid is GE varnish 7031, purchased from CMR-Direct, Somersham, United Kingdom and was chosen for its good mechanical strength at cryogenic temperatures. The thermal conductivity of GE varnish 7031 is 100 times lower than that of copper [28][29]. Therefore, it is important that there is no glue in between thermocouple and EM-grid. Preliminary plunge experiments showed that a layer of approximately 50 μm of glue in between thermocouple and EM-grid resulted in measured cooling rates that were indistinguishable from cooling rates measured during plunging of a thermocouple surrounded by the same thickness layer of glue. These experiments conformed that the layer of glue between EM-grid and thermocouple should be minimized to acquire reliable data on the cooling rate of the EM-grid during plunging. Therefore, one lead of the thermocouple was manipulated through a grid hole adjacent to the centre of the EM-grid and pulled through until the thermocouple was inside the grid hole. Both leads were then pulled to the edge of the EM-grid pressing the thermocouple bead against the grid bar, see Fig. 3.2a. One Autogrid and two EM-grids (A and B) were prepared this way.

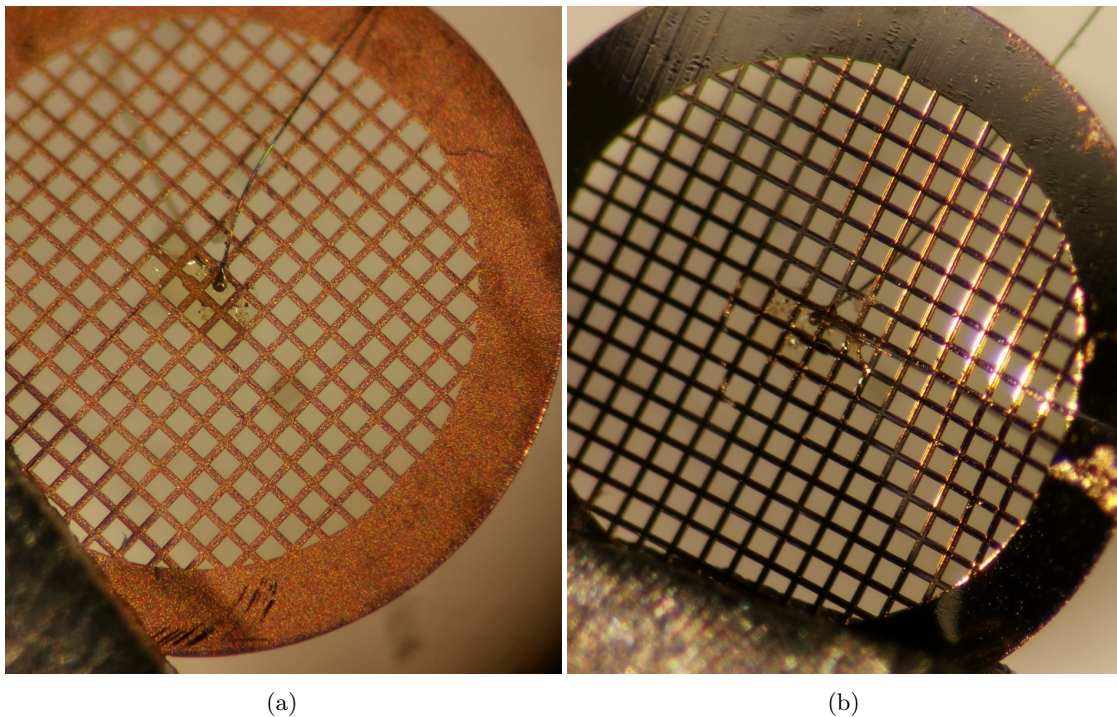
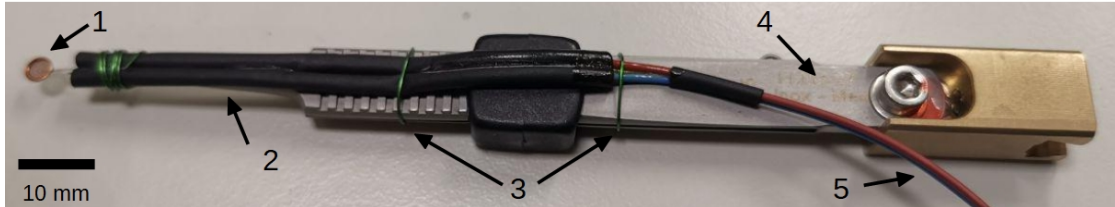


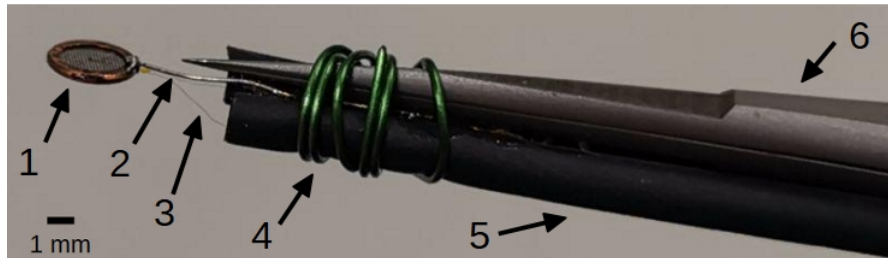
Figure 3.2: Thermocouple centred within 200 mesh copper EM-grid and covered with GE varnish 7031. (A). Front view (B). Back view.

Finally, a small dab of GE varnish 7031 diluted 1:1 with isopropanol 99.9% was deposited over the thermocouple from each side of the EM-grid securing the thermocouple in place. Furthermore, the

glue prevents direct contact between thermocouple and ethane, which would result in measured cooling rates that do not represent the cooling of the EM-grid. The thermocouples are fragile, and the wires tend to tangle making the fabrication process laborious and time consuming. The EM-grid with thermocouple was then attached to 26 AWG tinned copper insulated wire inside shrink tube, shown in Fig. 3.3a. The EM-grid was soldered to a 34 AWG tinned copper wire for ease of handling and attached to the Vitrobot plunge tweezers (see Fig. 3.3b).



(a) Measurement assembly on Vitrobot tweezers. (1) Autogrid with thermocouple (2) Shrink tube Steel wire lashing (3) Steel wire lashing (4) Vitrobot plunge tweezers (5) Signal wire to microcontroller



(b) Detail of Autogrid attached to tweezers Vitrobot tweezers. (1) Autogrid with thermocouple (2) 26 AWG tinned copper wire soldered to Autogrid and glued to shrink tube (3) 13 μm thermocouple wire (4) Steel wire lashing (5) Shrink tube (6) Vitrobot plunge tweezers

Figure 3.3: (a) Autogrid with thermocouple and wires strapped to plunge tweezers of the Vitrobot. (b) Detail of Autogrid on the tip of the tweezers. The Autogrid is soldered to a 34 AWG wire that is glued to the shrink tube.

Vitrobot setup

All plunge experiments were conducted using the FEI Vitrobot Mark IV. The settings of the vitrobot are shown in Table 3.1. Mounting the EM-grid and thermocouple assembly to the Vitrobot plunge tweezers was done by winding 26 AWG green painted steel wire around it, see Fig. 3.3b. The insulated wire was thread up through the bottom hole in the Vitrobot passed the plunge rod and then out through the side hole. Enough slack was left in the wire so the plunge rod could fully extend without straining the wire.

Data acquisition hardware

The thermocouple was connected to an AD8495 analog thermocouple amplifier (Adafruit, New York). Which in turn was connected to a NodeMCU ESP32 microcontroller (Joy-It, Neukirchen-Vluyn). The microcontroller was connected to a laptop via USB. The conversion time of the ADC on the microcontroller was 30 μs , resulting in a sampling rate of 32×10^3 samples per second. The available DRAM on the microcontroller limited the amount off samples stored to 55×10^3 and

Setting	Value
Temperature [C]	22
Humidity [s]	Off
Blot Time [s]	0.0
Drain Time [s]	0.0
Blot Force	0
Blot Total	0
Skip Application	No
Use Footpedal	Yes
Humidifier Off During Process	Yes
Skip Grid Transfer	Yes
Autorange Ethanolift	No

Table 3.1: Settings of the Vitrobot used during plunge freezing experiments

thus the recording time to 1.7s. For calibration and general temperature measurements a Pt1K platinum temperature sensor (TESLA BLATNÁ, Blatná) in a voltage divider circuit was used (see Fig. 3.4). The V_{out} is connected to a analog pin of the microcontroller.

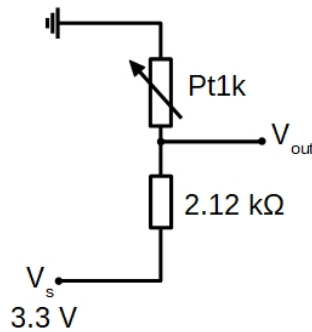


Figure 3.4: Schematic of the voltage divider circuit with the Pt1k platinum temperature sensor. The V_{out} was connected to an IO-pin of the microcontroller.

Data acquisition software

Data acquisition is done using three software programs. The microcontroller uses an Arduino IDE (Arduino, Somerville), program to read the voltage on the IO-pins, store the voltage data in an array, and send the data via the serial bus to the laptop. On the laptop a Python script (Python Software Foundation, Wilmington), runs to interact with the microcontroller over the serial bus. To start the measurement, a start-command was sent to the microcontroller that triggers the reading of voltages. When the reading was finished and the data was sent by the microcontroller, the Python script read the data from the serial bus and stored it in a CSV file on the Laptop. The data was then analysed by loading the CSV in MATLAB (MathWorks, Natick), where the voltage output of the thermocouple was converted to temperature using the relation acquired by calibration. Next, the temperature data was plotted. If multiple measurements were plotted in a single figure, they were shifted in time so that all the cooling curves overlap in the same point. Additional data analysis showed that the temperature data was smoothed with

the MATLAB tool 'smoothdata' [30]. The method used was 'rloess,' which is a robust quadratic regression over each window of the data array. The 'SmoothingFactor' was set to 0.01 to adjust the level of smoothing by scaling the heuristic window size.

Calibration

The thermocouple was calibrated using Pt1K platinum temperature sensor. Both sensors were glued to a 5 mm diameter nylon rod using GE varnish 7031. The rod was then placed in a 40 mL stainless steel cup insulated with Polystyrene holding 20 mL cooling liquid (see Fig. 3.5). Propane was used to measure temperature in the range 90 K to 230 K and Acetone in the range 190 K to 280 K. The measurement in propane was done three times. It took about 15 minutes for the propane and acetone to heat up. After the plunge experiments, the Autogrid and EM-grids were clamped to the nylon rod with Pt1K temperature sensor glued to it. Temperature and voltage was recorded while the grids were being dipped in LN2 and liquid propane and held in air.

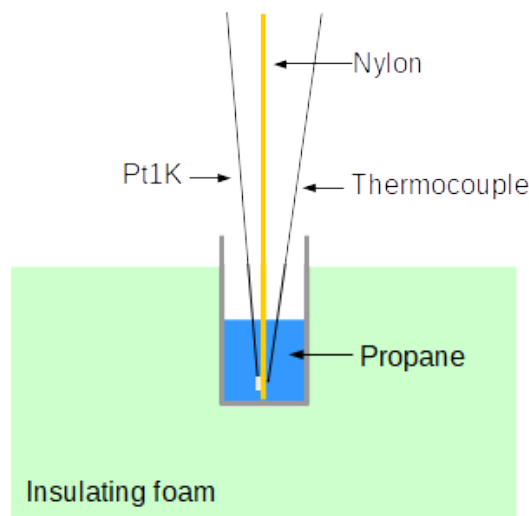


Figure 3.5: Sketch of the cross section of setup used for calibration.

Plunge speed measurement

The speed at which the Vitrobot plunges samples into cryogen was attained from high speed footage. Three recordings of the plunge motion were made at 235 FPS. The footage was analyzed using Tracker Video Analysis and Modelling Tool (Open Source Physics) and the motion visualized using MATLAB.

3.2.2 Model

In order to get an idea of the thermal response during plunging a Finite Element model, FEM, was made using COMSOL Multiphysics 5.4. Both EM-grid and Autogrid were modelled with in identical models where only the geometry was changed. The model uses a 3D heat transfer in solids module and a time depended solver. The geometries are imported from Solidworks models of the EM-grid and Autogrid with a grid mesh size of 400. The material for all bodies were copper selected from the build in material library. The plunging in cryogen was modelled with a

time and spacial dependent boundary condition on the surfaces of the EM-grid and Autogrid that were assumed to be in contact with the cryogen (see Fig. 3.6). In the first iteration of the model a temperature boundary condition was used where the temperature was constant (90 K) for a certain area. This area was changed in time to simulate the area that would be submerged. In the second iteration a similar boundary condition was used but with a constant convective heat transfer coefficient governing the heat load on the submerged area. All other surfaces were set to be thermally insulated. The initial temperature was set to 300 K. The mesh size was set to fine and the time depend solver was set to 40 us with 20 time-steps.

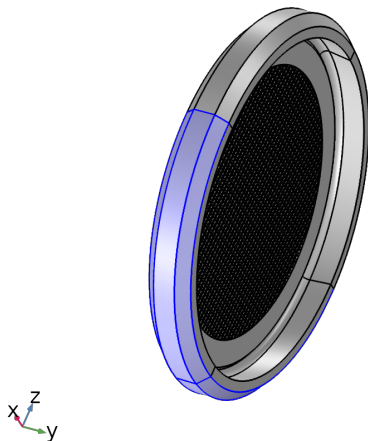


Figure 3.6: Surface of the Autogrid that was assumed to be in contact with the cryogen.

3.3 Results

3.3.1 Calibration

A relation was found between the thermocouple output voltage and temperature measured with the Pt1k temperature sensor during the calibration described in Chapter 3.2.1 that corresponded to the expected relation from literature [31] and is shown in Fig. 3.7. The relation from literature was shifted in voltage to overlap the calibration data. The three measurements in propane were coherent and followed the curve of the data from literature up to 900 mV, after which the experimental data showed less steep increase in temperature of voltage. The measurement in LN2 was in line with the ones in propane and the data from literature. The measurement in acetone did not match the ones in propane in the range where they overlap, 190 K to 230 K. The offset was 2 K to 5 K. However, the acetone measurement did correspond to the data from literature from 225 K onward. Data from the Autogrid and EM-grids is plotted as an error bar of the mean value over time for each medium (LN2, propane and air). At 300 K the data corresponded well with the data from literature but not in the temperature range below 150 K. Full calibration of the EM-grids and Autogrid will be performed to reduce the error in conversion.

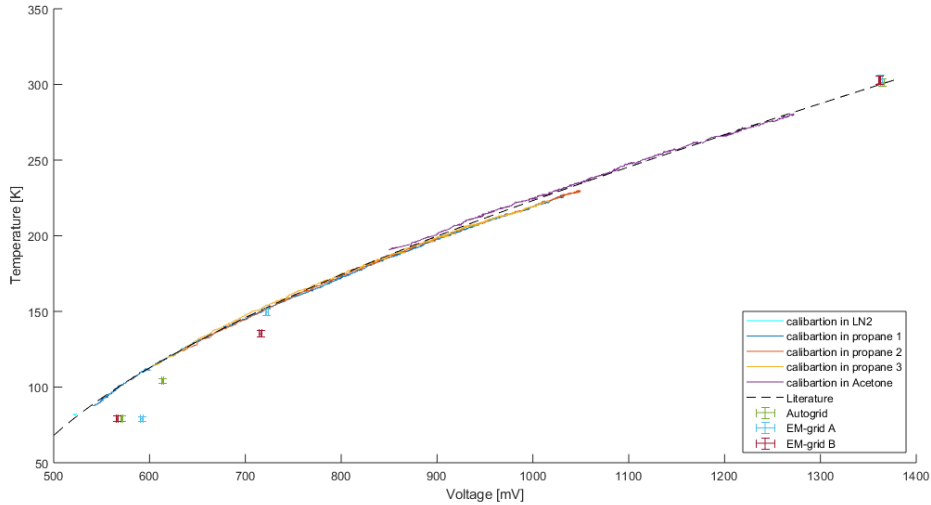


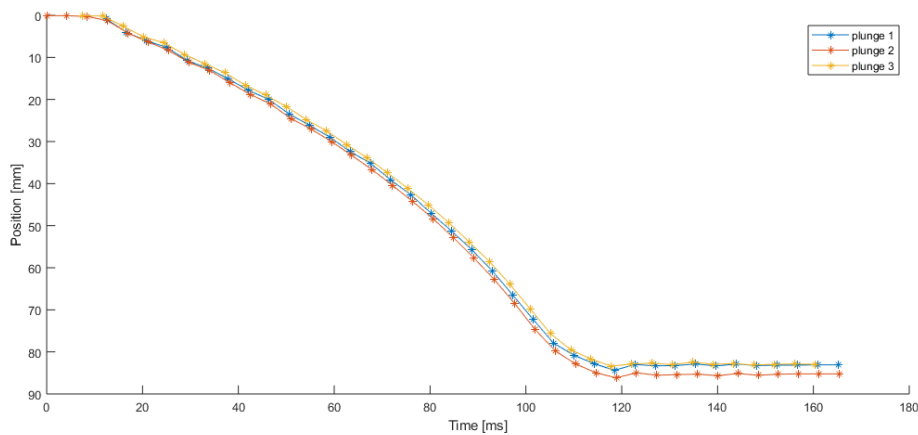
Figure 3.7: Temperature measure with the Pt1k plotted against output voltage of the thermocouple. Voltage of the solid line was measured with a bare TC as described in Chapter 3.2.1. Striped line shows relation from literature for a K-type thermocouple [31]. Striped line was shifted in voltage to best fit the calibration data. Measurements of Autogrid, EM-grid A and EM-grid B dipped in LN2 and propane and hold in air are shown with error bars.

3.3.2 Plunge speed measurement

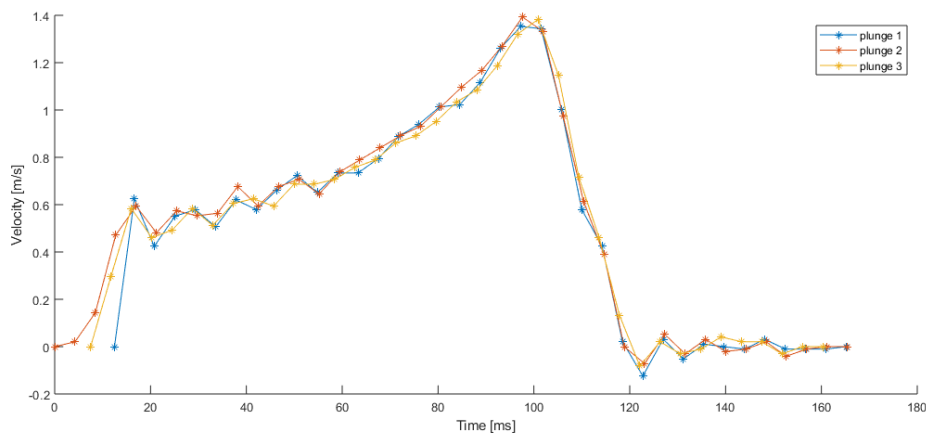
The vertical position and velocity of the Vitrobot tweezers during three plunges are shown in Fig. 3.8. The maximum speed reached by the Vitrobot tweezers was approximately 1.4 m s^{-1} at $t = 100 \text{ ms}$, where t was the time from start of the plunge. The maximum position was 85 mm at $t = 120 \text{ ms}$. At $t = 100 \text{ ms}$ the position was 70 mm. To determine the position of the tweezers relative to the ethane the cup holding the ethane was examined. The height of the copper cup holding ethane in which the tweezers plunge was 20 mm. The tweezers did not plunge all the way to the bottom of the cup. The tip of the tweezers stopped at 5 mm from the bottom. As a result, the tweezers travelled at maximum velocity when they entered the copper cup. The cup was generally filled with ethane for three-quarters or less, which is why the sample did not enter the ethane at maximum velocity. The lack of a constant speed at maximum velocity for a prolonged period, makes that having the ethane bath filled to the top is crucial for achieving maximum cooling rate. At the end of the stroke the tweezers bounced up slightly.

3.3.3 Cooling rate bare thermocouple

Four plunges of the same bare thermocouple in ethane were recorded, see Fig. 3.9. The data was shifted in time to intersect in 85 K. The measurements showed first a period of slow cooling trough the cold gas trapped above the ethane cup. After that followed a short period of rapid cooling at an average maximum rate of $2.3 \times 10^5 \text{ K s}^{-1}$. The start of rapid cooling marks the entering of ethane. The temperature at the beginning and end of the measurement and the maximum cooling rate are listed in Table 3.2. In the first plunge measurement the time between raising the ethane bath and plunging was more a 10 s. In the consecutive measurements the time was minimized to less than 5 s, to avoid nitrogen gas build up above the ethane bath. This is



(a)



(b)

Figure 3.8: Vertical position (a) and velocity (b) of the Vitrobot tweezers during plunging.

visible in the longer slow cooling period of plunge 1 in Fig. 3.9. The ethane was refrozen after the first and third plunge. This explains the difference in end temperature, specifically between the second and third plunge.

3.3.4 Cooling rate EM-grid and Autogrid

Four samples (EM-grid A, EM-grid B, Autogrid and bare thermocouple) were plunged in ethane while the temperature was recorded. The mean temperatures of the measurements of the samples is shown in Fig. 3.10. The data was shifted in time. The Autogrid was plunged on two separate days and those measurements are shown separately. From the measurements of Autogrid on day 1 only part of the data is included in Fig. 3.10. The reason why will be given in later paragraph. The recordings of each individual samples are show in Fig. 3.9 to 3.14. The measurements of the thermocouple showed first the slow cooling trough the cold gas above the ethane and then very rapid cooling when it enters ethane. Both the two EM-grid and the two Autogrid measurements

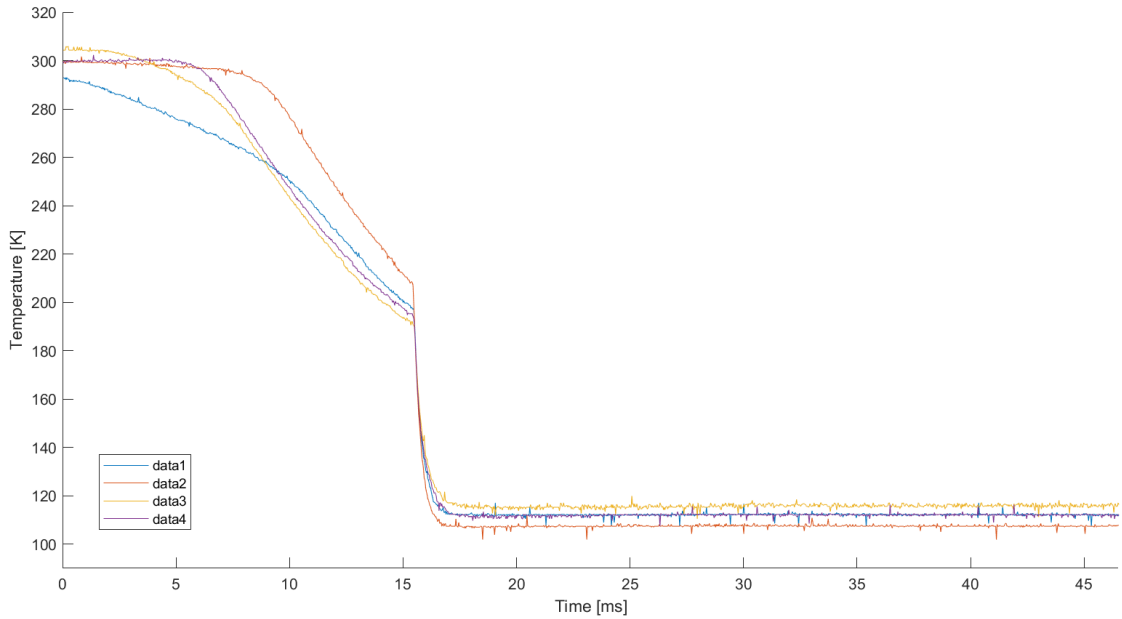


Figure 3.9: Cooling curves of bare thermocouple plunged in ethane.

	Begin temp. [K]	End temp. [K]	max dT/dt [Ks ⁻¹]
Plunge 1	301.8	131.4	2.25E+05
Plunge 2	302	137.7	2.69E+05
Plunge 3	307.2	125.8	2.26E+05
Plunge 4	301.9	118.8	2.30E+05

Table 3.2: Beginning and end temperatures and the maximum cooling rates of the measurements from the bare thermocouple.

show identical cooling rates up to 160 K. The Autogrid seemed to cool slower on average, but also reached a higher end temperature than the two EM-grids. Beginning and end temperatures and cooling rates are shown in Table 3.3

EM-grid A

EM-grid A was plunged 7 times, see Fig. 3.11. The data was shifted in time to intersect in 273 K. All measurements are comparable until 160 K. From there on irregular oscillation were measured. the average cooling rate from 273 K to 173 K was $6.4 \times 10^4 \text{ K s}^{-1}$. The beginning and end temperatures and cooling rate are listed in Table 3.4.

EM-grid B

There were six plunges performed with EM-grid B and their results are shown in Fig. 3.12 . These measurements were also shifted to intersect at 273 K. The cooling curves appear smooth with minimal oscillation compared to EM-grid B. A clear relation between end temperature and cooling rate can be seen, from looking at the data in Table 3.5: higher end temperature results

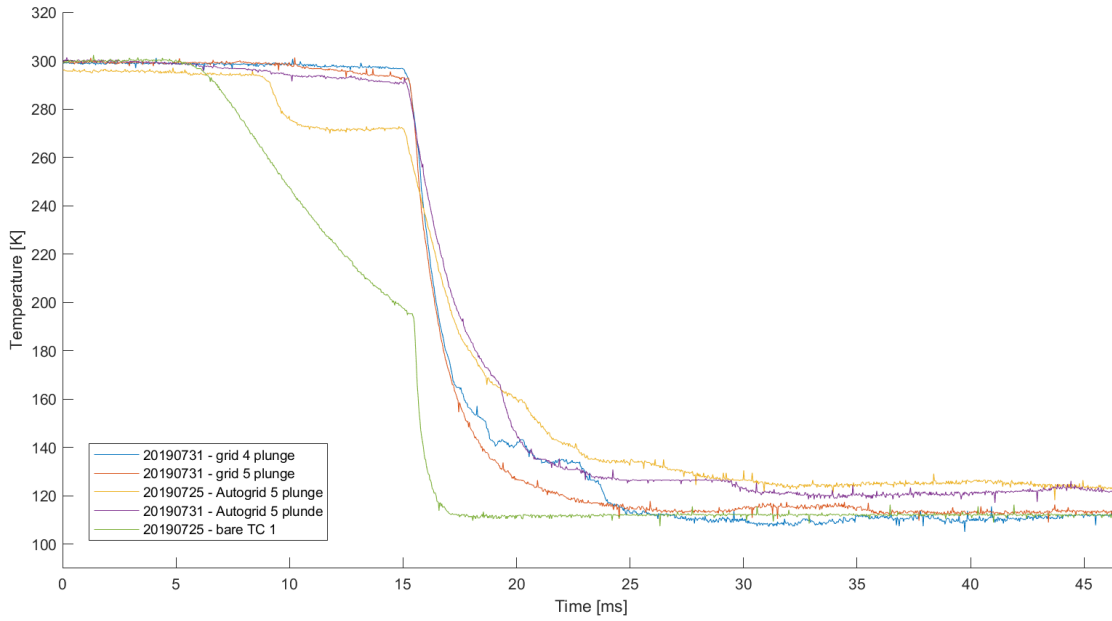


Figure 3.10

	N	Begin temp. (STD) [K]	End temp. (STD) [K]	Cooling rate 273 K – 173 K
Em-grid A	7	299.5 (1.07)	112.7 (2.88)	6.37E+04
Em-grid B	6	298.5 (1.50)	110.3 (5.41)	7.14E+04
Autogrid day 1	5*	298.4 (1.21)	116.1 (5.8)	3.36E+04
Autogrid day 2	5†	298.7 (1.45)	118.1 (3.69)	3.21E+04
Bare thermocouple	4	300.7 (3.4)	123.9 (7.85)	2.30E+05‡

Table 3.3: Average temperature at the beginning and end of the measurements of each sample and the cooling rates from 273 K to 173 K. * Plunges 6 to 10 were not included. † Plunges 6 to 8 were not included. ‡ Maximum dT/dt .

in a slower cooling rate. The variation in end temperature is a result of the refreezing after the third plunge, explaining the temperature rise from measurement 1 to 3 and from 4 to 6.

Autogrid day 1

The results of plunging the Autogrid on the day 1 are shown in Fig. 3.13 and Table 3.6. The data is shifted in time to intersect at 253 K. After the 5th plunge the Autogrid was dipped in LN2 for calibration purposes, together with the Pt1k temperature sensor. After this, the measurements showed unexpected slow cooling and heating between 300 K and 260 K. Therefore only the first five plunges were included in calculating the average temperatures in Fig. 3.10. The ethane was refrozen after plunges 3, 5, 7, and 9.

	Begin temp. [K]	End temp. [K]	Cooling rate 273 K – 173 K [Ks^{-1}]
Plunge 1	299.7	116.9	5.31E+04
Plunge 2	300.1	112.4	6.11E+04
Plunge 3	300.3	111	6.96E+04
Plunge 4	300.3	115.5	6.57E+04
Plunge 5	300	111.1	6.86E+04
Plunge 6	297.4	108.4	6.34E+04
Plunge 7	298.9	113.5	6.37E+04

Table 3.4: Beginning and end temperatures and the cooling rates of the measurements of EM-grid A.

	Begin temp. [K]	End temp. [K]	Cooling rate 273 K – 173 K [Ks^{-1}]
Plunge 1	299.2	101.7	8.10E+04
Plunge 2	296.5	112.7	6.74E+04
Plunge 3	296.2	117.9	5.77E+04
Plunge 4	299.9	106.4	7.88E+04
Plunge 5	299.3	107.5	6.65E+04
Plunge 6	299.6	112.4	7.14E+04

Table 3.5: Beginning and end temperatures and the cooling rates of the measurements of EM-grid B.

	Begin temp. [K]	End temp. [K]	Cooling rate 273 K – 173 K [Ks^{-1}]
Plunge 1	299.5	115	3.64E+04
Plunge 2	296.5	118.5	3.14E+04
Plunge 3	297.4	124.1	2.97E+04
Plunge 4	301.5	118.1	2.70E+04
Plunge 5	297.8	122.2	3.36E+04

Table 3.6: Beginning and end temperatures and the cooling rates of the measurements of the Autogrid on day 1.

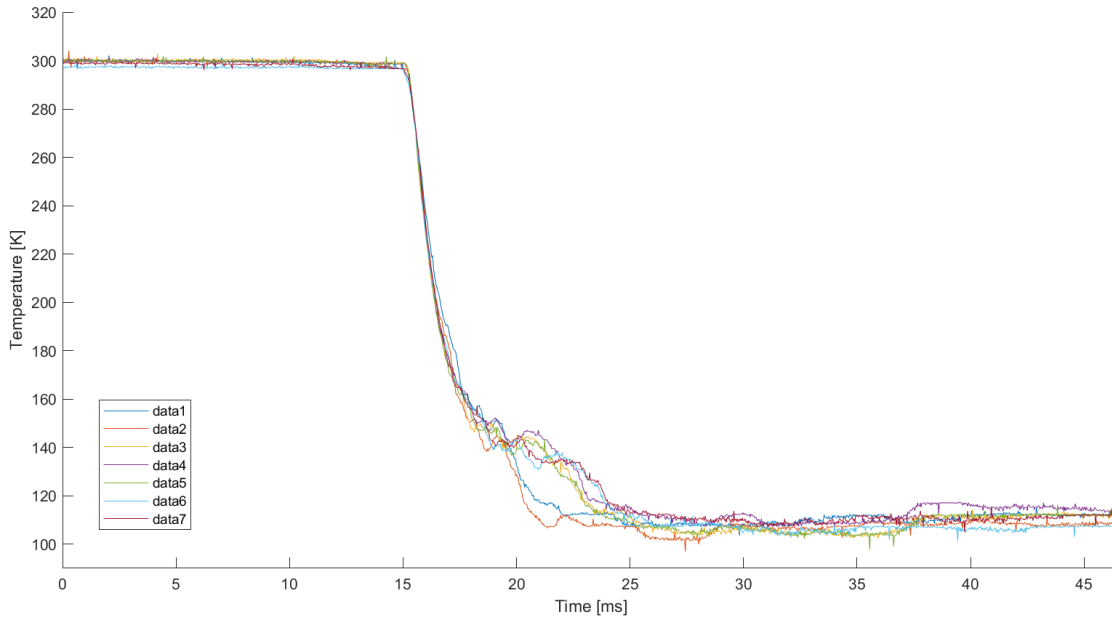


Figure 3.11: Cooling curves of EM-grid A plunged in ethane.

Autogrid day 2

Results from the second day of plunging the Autogrid are shown in Fig. 3.14 and Table 3.7. The data is shifted in time to intersect at 283 K. After the fifth plunge the ethane cup was refilled because the ethane level seemed low. The refilling was inadequate since the ethane level was now lower than before. Plunges 6 to 8 show slower cooling rates. Plunges 6 and 7 show an identical increase in cooling rate at 185 K, where plunge 8 shows a similar increase in cooling rate at 165 K. This change in cooling rate is caused by transition of film boiling into nucleate boiling [6]. That this is apparent is also an indication of slow plunge speed. The ethane was refrozen after plunges 2, 5 and 7.

	Begin temp. [K]	End temp. [K]	Cooling rate 273 K – 173 K [Ks^{-1}]
Plunge 1	298.9	117	4.61E+04
Plunge 2	299.3	119	4.94E+04
Plunge 3	300.1	116.2	4.68E+04
Plunge 4	298.1	115.1	5.91E+04
Plunge 5	298	116.7	5.17E+04
Plunge 6	299.4	120	3.14E+04
Plunge 7	295.6	126.1	3.08E+04
Plunge 8	300	114.8	3.21E+04

Table 3.7: Beginning and end temperatures and the cooling rates of the measurements of the Autogrid on day 2.

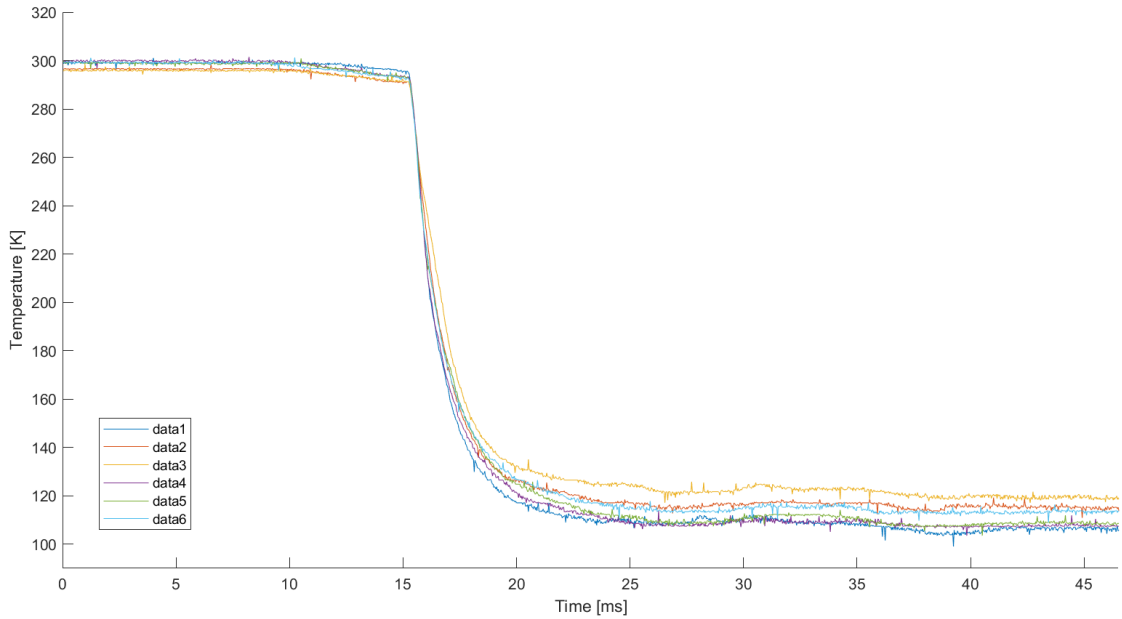


Figure 3.12: Cooling curves of EM-grid B plunged in ethane.

3.3.5 Convective heat transfer coefficient

To calculate the convective heat transfer it is important to know the initial temperature of the ethane. Since this was not measured an estimated guess must be made. The plunges that are likely to have had similar ethane temperatures are the ones right after refreezing, from the EM-grid and thermocouple. Their average temperature was $107.3K \pm 3.25K$. The standard deviation is similar to the measurement accuracy. This average temperature was used as initial temperature for calculating all heat transfer coefficients. The variation in temperature shown in a variation in heat transfer coefficient. Since the Autogrids never reached equilibrium and add significantly more heat to the ethane their temperatures should not be considered. This initial temperature and the cooling rates from Table 3.3 were used to calculate h with equation (3.3) and B_i with equation (3.1) and are shown in table 3.8. The Biot number of both the Em-grid and the Autogrid is much lower than 0.1, thus their cooling is convection limited. The cooling rate of the Autogrid was not as high as the EM-grid. The fact that the Autogrid cooled faster during the second day meant that it was convection limited on the first day. The conduction is only a function of the properties of the sample. Bald (1987)[6] gives the other methods of calculating the heat transfer convection in ethane. One is only dependent on plunge speed and derived from measurements done by Ryan (1987) [18]. The consideration for this relation was to take film boiling into account. Ryan (1991) [7] points out that this relation is in good agreement with experiments at 1.12 m/s but not anymore at 2.24 m/s. The second method is following empirical relations for forced convection that are dependent on Re and Pr. Results of both methods are also shown in Table 3.8

3.3.6 COMSOL model

Several thought experiments were checked with the COMSOL model. For instance what the influence of mesh size is on heat conduction through the grid. The difference in conductive cooling rate between a 400 and 200 mesh grid was 2.5%. The difference between a 200 mesh grid and a

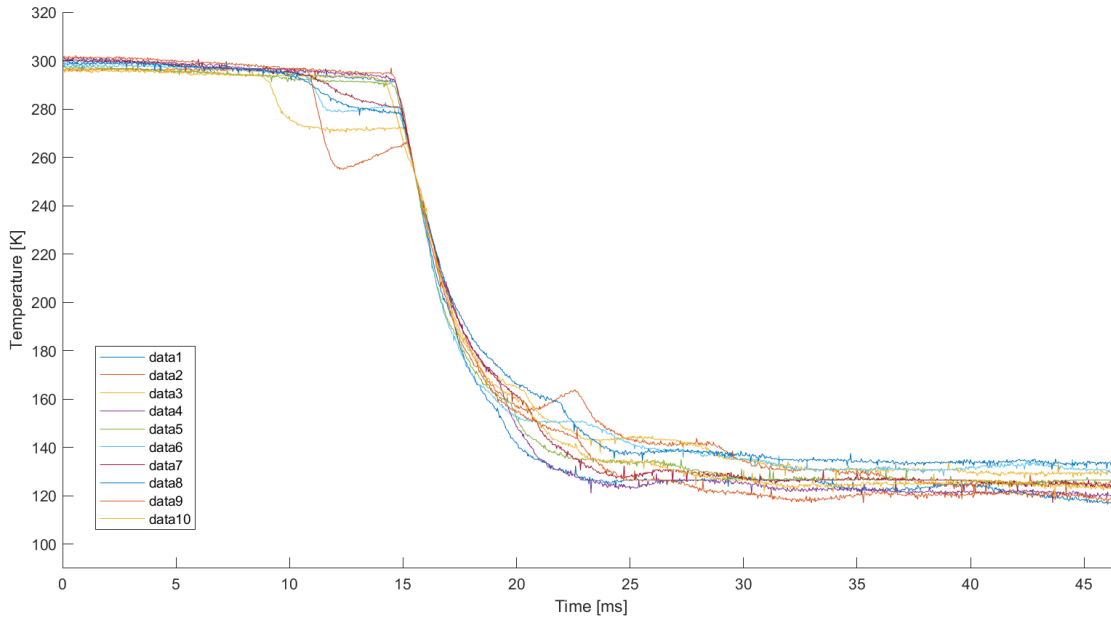


Figure 3.13: Cooling curves of Autogrid day 1 plunged in ethane.

solid copper disk of the same size was less than 10%. Additionally, the profile of the calculated convective heat transfer was used as a time dependent heat load in the COMSOL model on a solid 3 mm disk. The resulted cooling rate was faster in the first 10 ms of cooling but only reached a 140K after 50 ms.

	$h(T_{\infty} = 107.3K)$ [$W m^{-2} K^{-1}$] ($T_{\infty} \pm 3.25K$)
EM-grid A	28333 (1572)
EM-grid B	24989 (533)
Autogrid day 1	15053(1143)
Autogrid day 2	16423 (1532)
Thermocouple	22699 (3134)
$h(V)$	8868
$h(Re,Pr)$	5688

Table 3.8: Heat transfer coefficient calculated using the lumped thermal capacity model and the average temperatures of EM-grids, Autogrid and thermocouple. T_{∞} was estimated as 107.3K. Variation in h due to a change in T_{∞} is shown between brackets. Bottom two rows show the heat transfer coefficient calculated from a relation with plunge speed and a relation with Re and Pr [6].

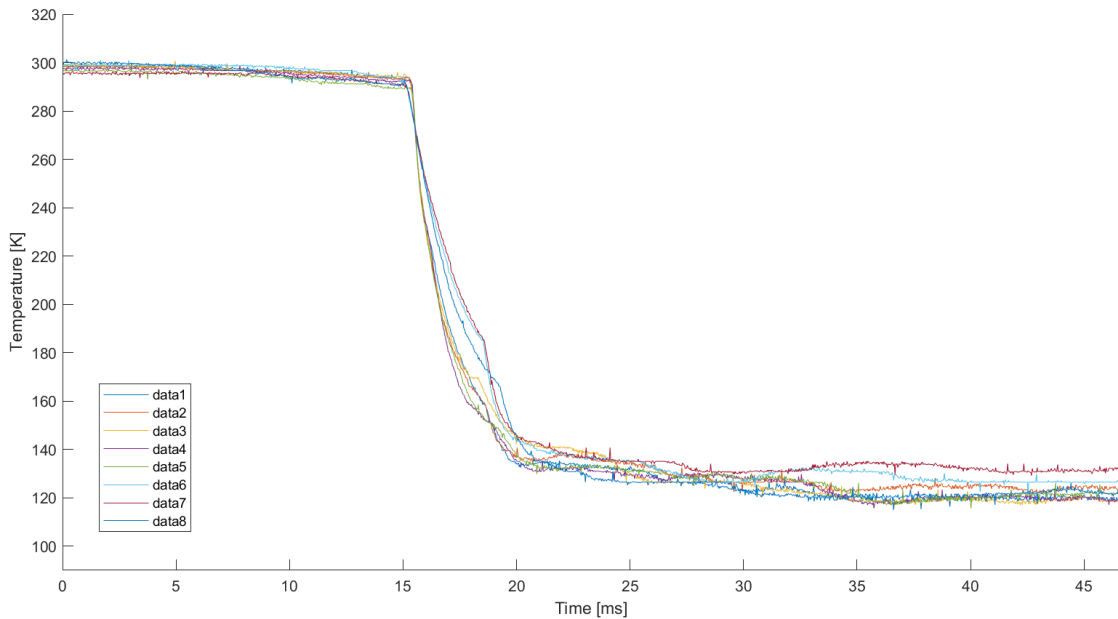


Figure 3.14: Cooling curves of Autogrid day 2 plunged in ethane.

3.4 Discussion

3.4.1 Experiments

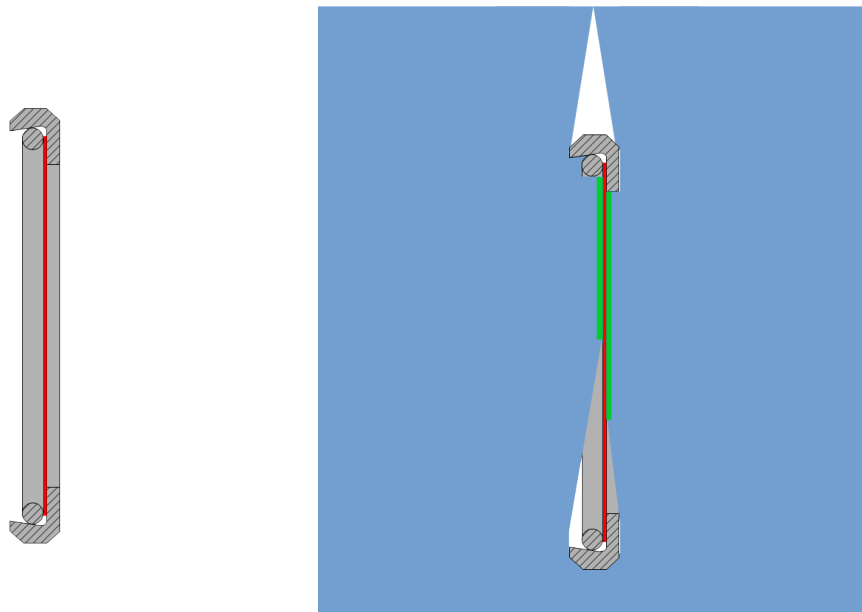
EM-grid wetting

Earlier in this paper the assumption was made that the faces of an EM-grid are not wetted by ethane when it enters ethane and only the outer rim is, as suggested by Kasas (2003). To figure out the proper way of mounting a thermocouple to the EM-grid a plunge measurement was performed with a thermocouple centered in the grid, as described in Chapter 3.2.1, but without glue on it. So this was a bare thermocouple nested in the center of the grid hold in place by tension on the thermocouple leads. The cooling rate measured from this sample was identical to that of just a bare thermocouple. This suggests that the face of the EM-grid was wetted by ethane. Another explanation would be that the surface is not wetted, but that the radiative heat transfer is as large as the convective heat transfer. The radiative heat transfer was approximated with the Stefan-Boltzmann's law for a small convex object:

$$Q_{12} = A_1 \epsilon_1 \sigma (T_1^4 - T_2^4) \quad (3.4)$$

Where Q is the heat transfer, $A_1 = 7.07 \times 10^{-6} \text{ m}^2$ is the area of the face of the EM-grid, $\epsilon_1 = 0.8$ is the emissivity of oxidized copper (one side of the EM-grid appeared black, see image 3.2a), $T_1 = 300 \text{ K}$ is the temperature of the EM-grid and $T_2 = 90 \text{ K}$ is the temperature of the ethane. This results in a radiative heat transfer of 2.6 mW. According to Bald (1985) [32] the convective heat transfer coefficient at 1 m s^{-1} in ethane would be about $2 \text{ kW m}^{-2} \text{ K}^{-1}$. For an EM-grid at 300 K and ethane at 90 K the convective heat transfer would then be 3 W. According to Silvester (1982) [33] the convective heat transfer coefficient of liquid ethane is between 1.5 and $5 \text{ kW m}^{-2} \text{ K}^{-1}$. The estimated radiative heat transfer is three orders smaller than the convective

heat transfer thus it is very unlikely that the fast cooling rate measure with the bare thermocouple centered in the EM-grid is a result of only radiative heat transfer. Therefore the faces of the EM-grid ethane must have been in direct contact with ethane. If this is also the case for the Autogrid can not be concluded from this. It can be expected that the difference in geometry creates a very different ethane flow around the Autogrid where the ethane does not touch one or both of the faces of the EM-grid inside the Autogrid. The Autogrid is $400\ \mu\text{m}$ thick which is 16 times thicker than an EM-grid, thus it displaces more fluid while plunging. Furthermore is the EM-grid inside the Autogrid not centered, see Fig.3.15a. Ethane might not enter the void on one side of the Autogrid, as illustrated in Fig. 3.15b.



(a) Cross section of the Autogrid. Support is shown in grey and EM-grid in red.

(b) Cross section of the Autogrid with possible ethane flow. Support is shown in grey, EM-grid in red, ethane in blue and wetted area in green.

Figure 3.15

Ethane temperature

The end temperature of a measurement (average of the last 200 out of 55000 data points) is not a good representation of the ethane temperature before plunging. Since the beginning of a measurement was manual triggered after the plunge sequence of the Vitrobot was started, variation exist in where in the measured 1.7 s the sample enters the ethane. Consequently the time that the sample was submerged at the end of the measurement also varies between measurements. During plunging the ethane is heated by both the sample and to a greater extent the mounting hardware. When the sample enters the ethane early in the measurement, the ethane will have a higher end temperature. This can be seen in the measurements of the bare thermocouple. Plunge 3 initially cools to a higher temperature than plunge 2, what is expected since it was the second plunge after freezing of the ethane thus the ethane was warmer during the third plunge. In contrary the end temperature of the third measurement is lower than the second measurement. Looking at the absolute times of both measurements confirmed this: during plunge

2 the ethane is entered 729 ms into the measurement and during plunge 3 961 ms. A more comparable temperature would be at a fixed time after plunge. The latest a plunge happened was 1.14 s after beginning the measurement, so the longest time all samples were measured after plunging was 580 ms. Though this temperature is comparable between measurements it is still not a good indication of the ethane temperature before cooling, because of the heating up of ethane overtime. A better indication of the ethane temperature before plunging would be the steady state temperature right after plunging, because in the short time after plunging the ethane locally around the sample is not yet heated by the mounting hardware. The steady state temperature was calculated from the average temperature 35 ms to 40 ms after entering the ethane, since this was the shortest time at which most measurements reached a steady state. For the Autogrid this is not a good indicator, because its temperature kept going down for at least 580 ms, thus it did not reach steady state within 40 ms. The best indication of the ethane temperature before plunging is the minimum temperature reached during the measurement. Prior to calculating the minimum of the temperature curve and smoothing operation was performed to remove noise from the curve. An example of a smoothed curve is shown in Fig. 3.16. The temperature after 40 ms and 580 ms and the minimum temperature of all measurements are shown in A.1.

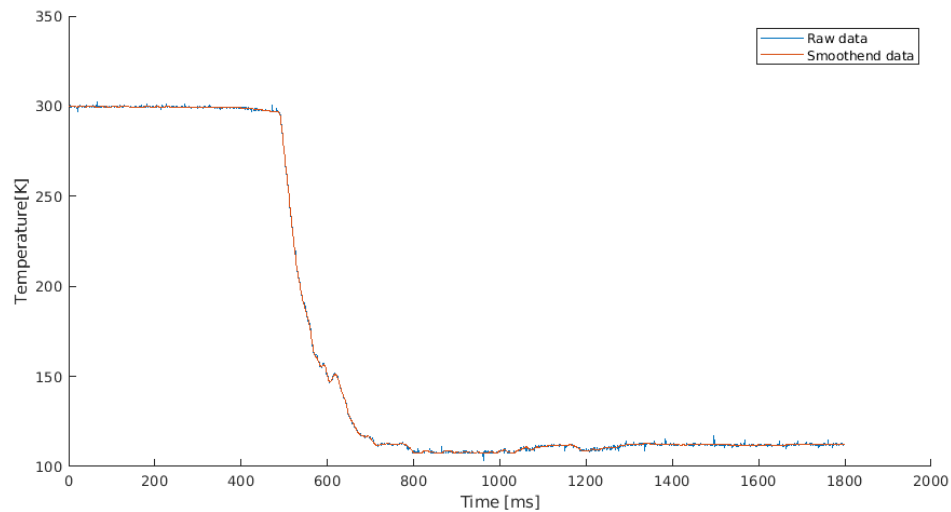


Figure 3.16: Example of raw data and smoothed data

Cooling rate as a function of the steady state temperature

The cooling rate is a function of the temperature of the ethane. Since the ethane was not at a constant temperature during all experiments and the exact temperature was not recorded, the cooling rates of the different plunges can not be directly compared. It is more relevant to evaluate the cooling rates as a function of the steady state temperature right after the plunge, as described in the previous section.

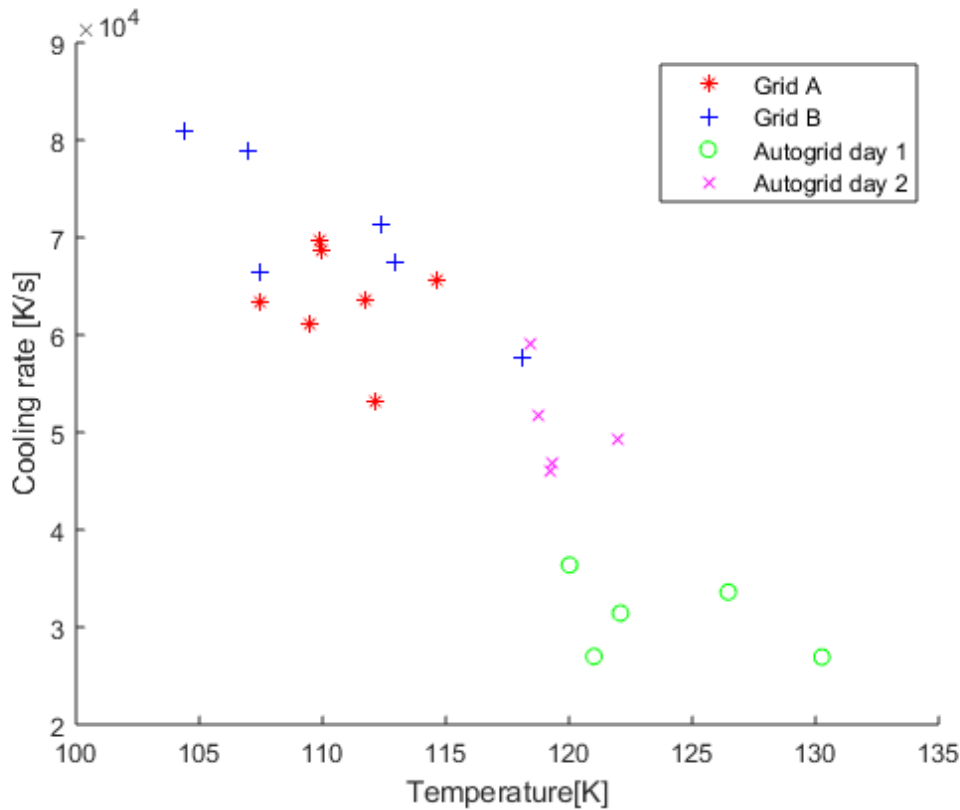


Figure 3.17: cooling rate vs end temp.

Increasing cooling rate of the Autogrid

As shown in Chapter 3.3.5 was the cooling rate of the Autogrid convection limited in the experiments. That means that there is the potential to increase the cooling rate without changing the material or geometry of the Autogrid. Increasing plunge velocity and plunge speed could improve cooling rate. Suppression of film boiling could be achieved by faster plunging or changing the surface roughness. The Autogrid also does not reach steady state even after more than a 1 s. This means that cooling is happening far after the forced convection has ended and that the Autogrid is being cooled by natural convection. There it was not convection limited and the longer plunging would increase the cooling rate.

3.5 Conclusion

This thesis has focused on understanding the thermodynamics of plunge freezing and applying that knowledge to the research of vitrification on an Autogrid in the Vitrobot. The experimental data that was acquired gave us new insight in the workings of the Vitrobot. The velocity profile of the plunge is a sharp peak, with a very short time of maximum velocity. Furthermore, the uncontrolled ethane bath results in large variation in cooling rate. For the first the cooling rate of EM-grids and Autogrid were recorded. Calculated Heat transfer coefficient confirms that cooling

during plunging is not convection limited. Higher cooling rate are thus possible when plunge velocity and plunge depth are increased. Vitrification of biological samples on an Autogrid was deemed unlikely with the Vitrtobot. Future research should consist of plunge freezing in a device with a controlled ethane bath, variable plunge speed where the samples travels at maximum velocity during the majority of the plunge and a deep bath. If Faster and deeper plunging would not result in a cooling rate fast enough for vitrification, then the geometry and material properties of the Autogrid have to be revised. Additional research could be done in the effectiveness of stirring the cryogen during plunging, to alter the flow characteristics that influence film boiling.

Chapter 4

Reflection

This chapter will reflect on the work and give a recommendation for future work.

4.1 Research focus

The initial scope of the research started very wide, with just the idea of improving the use of the Autogrid. The lack of knowledge on temperature changes and contamination during the cryo-EM workflow gave birth to the idea of incorporating a sensor inside the Autogrid. After three months of research a concept was presented of a surface acoustic wave temperature sensor build into an Autogrid. Unfortunately, the conclusion had to be drawn that further development would require extensive knowledge outside the writer's educational background. Additionally, research from fellow graduate student had resulted in an improved workflow where continuous sensing was less of a necessity. Several alternative improvements of the Autogrid were then considered. A notable concept was briefly investigated that focused on binary temperature sensing on the Autogrid as early failure detection. The goal would have been to make disposable Autogrid that would let the user know if devitrification had occurred. If this concept had come up during the initial phase of the research, it would have been a nice project to work on. None-the-less the current project was chosen to work on, partly because an experimental study seemed easier to structure within the given time frame.

4.2 Literature research

Literature research was conducted throughout the thesis research. At first it seemed there was not much published on measuring cooling rates. Especially in recent years. Only a handful of relevant papers were found from after the year 2000. The discovery of Ryan's dissertation (1991) led to many essential papers. His literature research was a great source of papers and books. For instance, Bald's Quantitative Cryofixation (1987) was a great book for theory on the thermodynamic processes during plunge freezing. Many interesting papers were published in the Journal of Microscopy. Unfortunately this journal was one of view only available in paper form at the TU Delft library and not for loan. This meant spending quite some time at the library photocopying. The data base of literature collected during the course of the research holds over 450 articles and 30 books.

4.3 Research approach

From the beginning the goal had been to measure the cooling rate of an Autogrid. Simply vitrifying an autogrid with the Vitrobot would make further automation of Cryo-EM workflow much easier that it was a surprise at first that no publications existed of the feasibility. From speaking to experts in the field it became clear that it probably wouldn't work, because it wasn't marketed by manufactures of plunge freezing devices. This notion was not regarded as a reason not to proceed. It did confine the optimistic expectation of the Autogrids capability to vitrify. Therefore more thought was put into possible improvement to current plunge freezing devices in general, ahead of the experiments.

4.4 Thermocouple fabrication

Rudimentary FEM analysis of the cooling of an EM-grid during plunge freezing predicted Cooling would be over in 20 ms. According to literature available at that time a 25 μm thermocouple would have a response time of 3 ms. This was motivation of using even finer thermocouples made from 13 μm diameter wire. This was the thinnest thermocouple wire available for purchase. So two 15m spools were ordered, which toke two weeks to be delivered. That time was partly spent on building the hardware for arc welding the thermocouples. The fabrication process was extremely finicky and had a high failure at the start. After two weeks only five thermocouples were fabricated and ready for testing. releasing many more would be needed, and production should be faster and improved version of the fabrication station was built that was designed with faster production and minimum wasted wire in mind. At this point half of the purchased wire had been used and delivery times had gone up to eight weeks, so ordering more was not an option. More thorough research on the supplier's website revealed that purchasing premade thermocouples of this size would have been possible on request. No delivery times were mentioned though and at a cost of €15 each it would have been much more expensive too. The second version of the fabrication station worked well, partly because it could be placed directly under the microscope form inspection of the weld. In the end the fabrication process had been optimized and if all went well three thermocouples could be welded and fully assembled in a day. primarily gluing the thermocouple to the EM-grid was done by dipping the thermocouple a view times in diluted varnish to create a thin sticky layer and then pressing the thermocouple onto the grid.

4.5 Experimental research

The first plunge experiment of an EM-grid seemed to go well. The data showed a beautiful cooling curve that was comparable to results from literature. Though electric noise was clearly visible in the results, it was not problematic. Attempts to reduce electric noise by adding small capacitors to the power source and readout pins were unsuccessful. On one occasion a thermocouple that had been clued to an EM-grid come lose while preparing for plunging. It was still functional but covered with varnish. Since the experiment was already set up, the thermocouple was plunged any way. The resulting cooling curve was practically indistinguishably from the earlier EM-grid cooling curve. Other EM-grids that had been plunged showed the same cooing rate as a bare thermocouple. Inspecting of the sample made so for confirmed what was suspected. The thermocouples were either some distance away from the grid with glue in between or they were poking through the grid and sticking out the other side, also some distance away from the grid. This meant that the method of gluing the thermocouple had to be revised. The new method of sort of weaving the thermocouple trough and pulling the bead against the grid bar showed good

thermal conduction between grid and bead. The varnish was also diluted more, and a smaller amount was applied. With regard to the Vitrobot MK IV, there are several things that could be improved upon: a velocity profile that is a short ramp and then a steady maximum velocity during the whole plunge instead of a short peak of maximum velocity, a deeper ethane bath such that deeper plunging would be possible and ethane level would be less of a factor in cooling rate and a temperature controlled ethane bath (which supposedly is already used in the newest version). The overall design turned out to be less thought through than beforehand was expected. The final thing that would have been advantageous is if the start of a measurement would have been triggered by the plunge and also high-speed footage was taken at the same time. Temperature data could then have been more easily correlated with position data and the time of entering the ethane.

4.6 Future work

The first thing that could be done differently to enhance the results is using the newer Leica plunge freezing device, since it has a temperature-controlled ethane bath. Additionally, measuring the ethane temperature with a small thermocouple would be advised. Better calibration of each sample would be useful. Measuring temperature gradients in the ethane bath would be interesting; there is reason to believe that there is significant temperature difference between the top and bottom of the ethane bath. Evidently more plunge experiments would better calibrated thermocouples would yield a smaller margin of error in the results. With Future plunge experiments it would also be advised to use a different plunge device, that can accommodate deeper and faster plunging, since the Autogrid is not limited by convection in the Vitrobot.

Appendix A

Table with measurement results

Appendix B

Software

B.1 Matlab code

```
1  clc
2  clear all
3  close all
4  %% data files
5  sample_size = 10;
6
7  right = 1300; %1300
8  left = 500; %88
9
10 T_inf = 100;
11 %%
12
13 %% load by folder
14 Subfolder_str = [...
15     "20190731 - grid 4 plunge "...
16     "20190731 - grid 5 plunge "...
17     "20190725 - Autogrid 5 plunge "...
18     "20190731 - Autogrid 5 plunde "...
19     "20190725 - bare TC 1"...
20 ];
21
22 set = 1;
23 for p = 1:length(Subfolder_str)
24
25     Subfolder = char(Subfolder_str(p));
26     %MatlabFolder = 'C:\Users\Thuis\Dropbox (DELMIC)\
27         Technology_Development\Cryo Transfer Graduation Projects\Bas\
28         Matlab\';
29     MatlabFolder = '/home/bas/Dropbox (DELMIC)/Technology_Development/
30         Cryo Transfer Graduation Projects/Bas/Matlab/';
31     FullFolderName = join ([MatlabFolder, Subfolder]);
```

```

29 filePattern = char(fullfile(FullFolderName, '*.csv'));
30 theFiles = dir(filePattern);
31 folder_name = strcat('folder_',int2str(p));
32
33 for k = 1 : length(theFiles)
34     baseFileName = theFiles(k).name;
35     file_names(p,k) = string(baseFileName);
36     plunge_name = strcat('plunge_',int2str(k));
37     data.(folder_name).(plunge_name) = [];
38 end
39 set = set +1;
40 data.(folder_name).name = Subfolder_str(p);
41 end
42 index = 1;
43 for q = 1:numel(fieldnames(data))
44     sample_number = q
45     %%
46     folder_name = strcat('folder_',int2str(q));
47     plunge_amount = numel(fieldnames(data.(folder_name)))-1;
48     %% create figure
49     figure('Position',[0,0,1200,600]) %500,300
50     hold on
51     %% figure style
52     %title(Subfolder_str(q))
53     legend('Units','pixels','Position',[230 (110+8*(plunge_amount-1)
54         ) 0 0]);
54     ylabel("Temperature [K]")
55     xlabel("Time [ms]")
56     axis([-inf inf 90 320]) %[0 inf 90 310]
57
58
59 %%
60 for n = 1:plunge_amount
61     plunge_number = n
62     %% import data
63     plunge_name = strcat('plunge_',int2str(n));
64
65     tabel_TC = csvread(file_names(q,n));
66     data_size = length(tabel_TC);
67     data.(folder_name).(plunge_name).TC_mV = tabel_TC(2:
68         data_size)';
69     TC_mV = data.(folder_name).(plunge_name).TC_mV;
70
71     data.(folder_name).(plunge_name).sample_time = tabel_TC(1);
72
73     % k_type_mV_amped_to_K
74     for i=1:length(TC_mV)
75         data.(folder_name).(plunge_name).TC_K(i) =
76             k_type_mV_amped_to_K(data.(folder_name).(plunge_name).

```

```

TC_mV(i));
75 end
76 TC_K = data.(folder_name).(plunge_name).TC_K;
77 %% simple average
78 sim = simple_average(TC_K,sample_size);
79 time_sim = [1:1:length(sim)].*0.031; % time in ms
80 diff_sim = abs(diff(sim));
81 [max_diff_sim_y,max_diff_sim_x] = max(diff_sim);
82
83 %% shorten & shift in x, sim data
84
85
86 % shift in x around max diff
87 %     if n == 1
88 %         range = [max_diff_sim_x(n)-left ,
89 %               max_diff_sim_x(n)+right];
90 %     else
91 %         y_sim_max(n) = sim(n,max_diff_sim_x(n));
92 %         x_sim_max_1 = get_x_for_y(sim(1,:),
93 %               y_sim_max(n));
94 %         corr = max_diff_sim_x(1)- x_sim_max_1;
95 %         range = [max_diff_sim_x(n)-left+corr ,
96 %               max_diff_sim_x(n)+right+corr];
97 %     end
98 % shift in x around 273 K
99 if Subfolder_str(q) == "20190725 - bare TC 1"
100     TC_K_x_273K_n = get_x_for_y(TC_K,185);
101 elseif Subfolder_str(q) == "20190712 - bare TC 1 plunge"
102     TC_K_x_273K_n = get_x_for_y(TC_K,220);
103 %elseif Subfolder_str(q) == "20190725 - Autogrid 5 plunge"
104 %    TC_K_x_273K_n = get_x_for_y(TC_K,253);
105 %elseif Subfolder_str(q) == "20190731 - Autogrid 5 plunge"
106 %    TC_K_x_273K_n = get_x_for_y(TC_K,285);
107 else
108     TC_K_x_273K_n = get_x_for_y(TC_K,273);
109 end
110 range = [TC_K_x_273K_n-left ,TC_K_x_273K_n+right];
111
112 plunge_moment(q,n) = TC_K_x_273K_n;
113
114 % create shortend arrays
115 %sim_short = sim(n,range(1):range(2));
116 data.(folder_name).(plunge_name).TC_K_short = TC_K(range(1):
117     range(2));
118 TC_K_short = data.(folder_name).(plunge_name).TC_K_short;
119 TC_K_short_array(n,:) = TC_K_short;
120
121 %% calculate diff TC_K data
122 diff_TC_K = abs(diff(TC_K));

```

```

119 [max_diff_TC_K_y,max_diff_TC_K_x] = max(diff_TC_K);
120 max_diff_TC_Ks = max_diff_TC_K_y/(31e-6); % [K/s] 31 us per
    sample
121 data.(folder_name).(plunge_name).max_diff_TC_Ks =
    max_diff_TC_Ks;
122
123 %% calculate begin an end temperature
124 K_begin = mean(TC_K(1:200));
125 K_begin_array(n) = K_begin;
126 data.(folder_name).(plunge_name).K_begin = K_begin;
127 K_end_measurement = mean(TC_K((length(TC_K)-200):length(TC_K)
    ));
128 K_end_array(n) = K_end_measurement;
129 data.(folder_name).(plunge_name).K_end_measurement =
    K_end_measurement;
130 K_end_measurement_table(q,n) = K_end_measurement;
131
132 % after 40 ms
133 K_end40 = mean(TC_K_short((left+1129):(left+1290))); %60 to
    62 ms ; 1330 - 1491 = 35 to 40 ms
134 K_end_array40(n) = K_end40;
135 data.(folder_name).(plunge_name).K_end40 = K_end40;
136
137 % after longest time for all measuermnets
138 time_long = TC_K_x_273K_n+18576;
139 K_end_long = mean(TC_K(time_long-322:time_long)); % 322
    samples is 10 ms
140 data.(folder_name).(plunge_name).K_end_long = K_end_long;
141 K_end_long_table(q,n) = K_end_long;
142
143 % mV
144 mV_begin = mean(TC_mV(1:200));
145 data.(folder_name).(plunge_name).mV_begin = mV_begin;
146 mV_end = mean(TC_mV((length(TC_K)-200):length(TC_K)));
147 data.(folder_name).(plunge_name).mV_end = mV_end;
148
149 % calculate cooling rate
150 cooling_rate_273_173 = cooling_rate(TC_K_short);
151 data.(folder_name).(plunge_name).cooling_rate_273_173 =
    cooling_rate_273_173;
152 cooling_rate_273_173_table(q,n) = cooling_rate_273_173;
153
154 %% smoothening
155 %smoothend = smooth(TC_K(TC_K_x_273K_n:length(TC_K)),0.01,'
    rloess');
156 smoothend = smooth(TC_K_short,0.01,'rloess');
157 data.(folder_name).(plunge_name).smoothend = smoothend;
158
159 %% minimum temperature

```

```

160     K_min = min(smoothend);
161     data.(folder_name).(plunge_name).K_min = K_min;
162     K_min_table(q,n) = K_min;
163     %% plot
164     time_TC_K_short = [1:1:length(TC_K_short)].*0.031-6.23; %
        time in ms
165     plot_style = '-';
166     plot(time_TC_K_short,TC_K_short,plot_style)% time_TC_K_short,
167     %plot(time_TC_K,smoothend,'--')
168
169     %           time_TC_K = [1:1:length(TC_K(n,:))].*0.031; % time
        in ms
170     %           plot_style = '-';
171     %           plot(time_TC_K,TC_K(n,:),plot_style)%
        time_TC_K_short,
172     %% save end40 and cooling rate in csv file
173     CR_end40_table(index,1) = data.(folder_name).(plunge_name).
        K_end40;
174     CR_end40_table(index,2) = data.(folder_name).(plunge_name).
        cooling_rate_273_173;
175     index = index +1;
176
177     %%
178     r_cyl = 3e-3;
179     r_sph = 20e-6;
180     h_plate = 20e-6;
181
182     var_dTdt = diff(data.(folder_name).(plunge_name).
        smoothend)/31e-6;
183     for z = 1:length(var_dTdt)
184         T = data.(folder_name).(plunge_name).smoothend(z); %
            [K]t temp between T_inf and T_i
185         dTdt = var_dTdt(z);
186         t_s = time_TC_K_short(z)/1000; % t is time interval
            needed for object to reach T from T_i
187
188         if folder_name == 'folder_5'
189             k_nickel = 2.7125e-08*T^4 + -3.3472e-05*T^3 +
                0.01544*T^2 + -3.2758*T + 367.94 ;
190             Cp_nickel = 1.3288e-05*T^3 - 0.012635*T^2 +
                4.3703*T -91.972;
191             k = k_nickel;%k_copper;
192             Cp = Cp_nickel;%Cp_copper;
193             Lc_sphere = r_sph/3; % a third of the radius
194             Lc = Lc_sphere;
195             rho_nickel = 8908; %[kg/m3]
196             rho = rho_nickel; %[kg/m3]
197         else

```

```

198         Cp_copper = 0.80952*T + 142.14; % 385 at 300K and
           215 at 90K
199         k_copper = -0.47143*T + 542.43; % 401 at 300K and
           500 at 90K
200         k = k_copper;%k_copper;
201         Cp = Cp_copper;%Cp_copper;
202         Lc_plate = h_plate/2; % half the thickness
203         Lc_cylinder = r_cyl/2; % half the radius
204         Lc = Lc_plate;
205         rho_copper = 8750; %[kg/m3]
206         rho = rho_copper;
207         end
208
209         h(z) = -dTdt*rho*Cp*Lc/(T-T_inf);
210         Bi(z) = (h(z)*Lc)/(k); % Bi always smaller the 1e-3
211         end
212
213         data.(folder_name).(plunge_name).Bi_max = max(Bi);
214         data.(folder_name).(plunge_name).h = h;
215
216
217
218     end
219
220
221 %% calculate mean and STD - TC_K_short
222 for j = 1:length(data.(folder_name).(plunge_name).TC_K_short) %
           length(TC_K_short(1,:))
223     mean_TC_K_short(j) = mean(TC_K_short(:,j));
224     STD_TC_K_short(j) = std(TC_K_short(:,j));
225 end
226 data.(folder_name).mean_TC_K_short = mean_TC_K_short;
227 data.(folder_name).STD_TC_K_short = STD_TC_K_short;
228
229 data.(folder_name).cooling_rate_273_173 = cooling_rate(
           mean_TC_K_short);
230 %% smoothening
231 smoothend_mean = smooth(mean_TC_K_short,0.01,'rloess');
232 data.(folder_name).smoothend_mean = smoothend_mean;
233
234 %% plot errorbar
235 % figure
236 % hold on
237 % title(file_names(q,1))
238 % time_mean_TC_K_short = [1:1:length(mean_TC_K_short(1,:))
           ].*0.031; % time in ms
239 % errorbar(time_mean_TC_K_short,mean_TC_K_short(q,:),
           STD_TC_K_short(q,:))
240 % ylabel("Temperature [K]")

```

```

241 % xlabel("Time [ms]")
242
243 %% mean and std from begin and end K and mV
244 data.(folder_name).K_begin_mean = mean(K_begin_array);
245 data.(folder_name).K_begin_std = std(K_begin_array);
246 data.(folder_name).K_end_mean = mean(K_end_array);
247 data.(folder_name).K_end_std = std(K_end_array);
248 %%
249 r_cyl = 3e-3;
250 r_sph = 20e-6;
251 h_plate = 20e-6;
252
253 var_dTdt = diff(data.(folder_name).smoothend_mean)/31e-6;
254 for w = 1:length(var_dTdt)
255     T = data.(folder_name).smoothend_mean(w); % [K]t temp
256         between T_inf and T_i
257     dTdt = var_dTdt(w);
258     t_s = time_TC_K_short(w)/1000; % t is time interval
259         needed for object to reach T from T_i
260
261     if folder_name == 'folder_5'
262         k_nickel = 2.7125e-08*T^4 + -3.3472e-05*T^3 +
263             0.01544*T^2 + -3.2758*T + 367.94 ;
264         Cp_nickel = 1.3288e-05*T^3 - 0.012635*T^2 +
265             4.3703*T - 91.972;
266         k = k_nickel;%k_copper;
267         Cp = Cp_nickel;%Cp_copper;
268         Lc_sphere = r_sph/3; % a third of the radius
269         Lc = Lc_sphere;
270         rho_nickel = 8908; %[kg/m3]
271         rho = rho_nickel; %[kg/m3]
272     else
273         Cp_copper = 0.80952*T + 142.14; % 385 at 300K and
274             215 at 90K
275         k_copper = -0.47143*T + 542.43; % 401 at 300K and
276             500 at 90K
277         k = k_copper;%k_copper;
278         Cp = Cp_copper;%Cp_copper;
279         Lc_plate = h_plate/2; % half the thickness
280         Lc_cylinder = r_cyl/2; % half the radius
281         Lc = Lc_plate;
282         rho_copper = 8750; %[kg/m3]
283         rho = rho_copper;
284     end
285
286     h(w) = -dTdt*rho*Cp*Lc/(T-T_inf);
287     h_CR = -dTdt*rho*Cp*Lc/(T-T_inf);
288     Bi(w) = (h(w)*Lc)/(k); % Bi always smaller the 1e-3
289 end

```

```

284
285         data.(folder_name).Bi_max = max(Bi);
286         data.(folder_name).h = h;
287
288     end
289
290     %% plot mean
291
292     % shift means
293
294     % plot
295     figure('Position',[0,0,1200,600]) %500,300
296     hold on
297     %time_mean_TC_K_short = [1:1:length(data.(folder_name).
298         mean_TC_K_short)].*0.031; % time in ms
299     for q = 1:numel(fieldnames(data))
300         folder_name = strcat('folder_',int2str(q));
301         plot(time_TC_K_short,data.(folder_name).mean_TC_K_short)
302     end
303
304     %% COMSOL rim only
305     % tabel_COMSOL_rim = csvread("Model_4_TEM-grid+TC_295K.csv",5);
306     % time_COMSOL_rim = tabel_COMSOL_rim(:,1)*1000;
307     % TC_K_COMSOL_rim = tabel_COMSOL_rim(:,2);
308     %
309     % plot(time_COMSOL_rim,TC_K_COMSOL_rim,'--')
310     %
311     %% COMSOL rim + side rim
312     % tabel_COMSOL_rimside = csvread("Model_4_TEM-grid+
313         TC_295K_side_rim_contact.csv",5);
314     % time_COMSOL_rimside = tabel_COMSOL_rimside(:,1)*1000;
315     % TC_K_COMSOL_rimside = tabel_COMSOL_rimside(:,2);
316     %
317     % plot(time_COMSOL_rimside,TC_K_COMSOL_rimside,'--')
318
319     %% figure style
320     %title('Grids and Autogrids overlaid')
321     legend(Subfolder_str,'Location','none','Position',[0.15 0.15 0.1750
322         0.1433]); %"experiment","COMSOL rim only","COMSOL rim + side rim"
323     ylabel("Temperature [K]")
324     xlabel("Time [ms]")
325     axis([-inf inf 90 320]) %[0 inf 90 310]
326
327     %% save data grid 5
328
329     save data.mat

```

B.2 Python code

```

1 import csv
2 import serial
3 import time
4 import _thread as thread
5 import numpy as np
6 import matplotlib.pyplot as plt
7 import math
8
9 file_name_base = "TC_experiment_"
10 file_name_extension = ".csv"
11
12
13
14 ser = serial.Serial("COM5", 115200, timeout=5)
15 time.sleep(1)
16 ser.flushInput()
17
18 def key_capture_thread():
19     while True:
20         input_ter = input()
21         if input_ter == "b":
22             #print("b received")
23             ser.write(input_ter.encode())
24         elif input_ter == "e":
25             #print("e received")
26             ser.write(input_ter.encode())
27
28 thread.start_new_thread(key_capture_thread, ())
29
30 def plot(TC_mV):
31     len_TC_mV = len(TC_mV)
32     growing_array = list(range(len_TC_mV))
33     numpy_array = np.array(growing_array)
34     time = numpy_array*0.031
35     plt.plot(time, TC_mV)
36     plt.title('Thermocouple plunged with Vitrobot')
37     plt.ylabel('Voltage [mV]')
38     plt.xlabel('Time [ms]')
39     plt.show()
40
41
42
43 while True:
44
45     try:
46         decoded_string = ser.readline().decode("ascii")
47         striped_decoded_string = decoded_string.strip().rstrip()
48         # if (striped_decoded_string[0]>='0') and (
49             striped_decoded_string[0]<='9'):

```

```

49     #     try:
50     #         TC_mV_temp = int(striped_decoded_string.rstrip())
51     #         print(TC_mV_temp)
52     #     except:
53     #         print("failed to read TC_mV from string: ",
54     #               striped_decoded_string.rstrip())
55     #         break
56     if striped_decoded_string in ["x"]:
57         print("file started")
58         TC_mV = []
59         try:
60             time_string = time.strftime("%Y%m%d-%H%M%S")
61             full_file_name = file_name_base + time_string +
62                 file_name_extension
63             f = open(full_file_name, "a")
64         except:
65             print("failed to create file name")
66             break
67         reading_file = True
68         while reading_file:
69             decoded_string = ser.readline().decode("ascii")
70             striped_decoded_string = decoded_string.strip()
71             if striped_decoded_string in ["y"]:
72                 reading_file = False
73                 print("file ended")
74                 f.close()
75                 del TC_mV[0]
76                 plot(TC_mV)
77             else:
78                 TC_mV_temp = int(striped_decoded_string.rstrip())
79                 TC_mV.append(TC_mV_temp)
80                 writer = csv.writer(f, delimiter=',', escapechar=
81                     ' ', quoting=csv.QUOTE_NONE)#, delimiter=",",
82                     quoting=csv.QUOTE_NONE)
83                 writer.writerow([striped_decoded_string.rstrip()
84                                 ])
85     except:
86         print("main loop failed")
87         break

```

B.3 Arduino code

```

1 #include "driver/adc.h"
2 #include "esp_adc_cal.h"
3 #include "SPIFFS.h"
4 #define size_of_data 55500
5 uint16_t array1[size_of_data];
6

```

```

7 char incomingChar;
8 bool measure = false;
9
10 // RTD_K coefficients
11 const float R2 = 2140;
12 const float Vin = 3.3 ;
13 const float RTD_a = -5.3117*pow(10,-9);
14 const float RTD_b = 2.4274*pow(10,-5);
15 const float RTD_c = 0.2232;
16 const float RTD_d = -242.15;
17
18 // define characterize ADC
19 #define REF_VOLTAGE 1114
20 esp_adc_cal_characteristics_t *adc_chars = new
    esp_adc_cal_characteristics_t;
21
22 uint16_t *read_sensor(uint16_t array2[size_of_data]){
23     int temp;
24
25     for (int k = 0; k < size_of_data; k++) {
26         adc2_get_raw( ADC2_CHANNEL_6, ADC_WIDTH_12Bit, &temp); //GPIO
27             14 = ADC2_CH6
28         //temp = k*2;
29         array2[k] = temp;
30     }
31     return array2;
32 }
33 void send_data(uint16_t array4[], int sample_time){
34     Serial.println("x");
35     Serial.println(sample_time);
36     for (int n = 0; n < size_of_data; n++) {
37         uint16_t TC_mV = esp_adc_cal_raw_to_voltage(array4[n], adc_chars)
38             ;
39         Serial.println(TC_mV);
40     }
41     Serial.println("y");
42 }
43 float measure_RTD(){
44     int read_raw_RTD;
45     adc2_get_raw( ADC2_CHANNEL_3, ADC_WIDTH_12Bit, &read_raw_RTD);
46     float RTD_vol_mV = esp_adc_cal_raw_to_voltage(read_raw_RTD,
47         adc_chars);
48     float RTD_vol_V = RTD_vol_mV * 0.001;
49     float RTD_ohm = Vin*R2/(Vin-RTD_vol_V)- R2;
50     float RTD_C = RTD_a*pow(RTD_ohm,3) + RTD_b*pow(RTD_ohm,2) + RTD_c
        *RTD_ohm + RTD_d;
51     float RTD_K = RTD_C + 273;

```

```

51     return RTD_K;
52
53 }
54
55 void handleSerial() {
56     while (Serial.available() > 0) {
57         char incomingChar = Serial.read();
58
59         switch (incomingChar) {
60             case 'b':
61                 measure = true;
62                 break;
63             case 'e':
64                 measure = false;
65                 break;
66         }
67     }
68 }
69
70 // setup
71 void setup() {
72     // set baud speed
73     Serial.begin(115200);
74
75     // configure ADC2
76
77     //adc2_config_channel_atten(ADC2_CHANNEL_3, ADC_ATTEN_DB_11); //
78     GPIO 15 = ADC2_CH3
79     //adc2_config_channel_atten(ADC2_CHANNEL_4, ADC_ATTEN_DB_11); //
80     GPIO 13 = ADC2_CH4
81     //adc2_config_channel_atten(ADC2_CHANNEL_5, ADC_ATTEN_DB_11); //
82     GPIO 12 = ADC2_CH5
83     adc2_config_channel_atten(ADC2_CHANNEL_6, ADC_ATTEN_DB_11); //GPIO
84     14 = ADC2_CH6
85
86     // characterize ADC2
87     esp_adc_cal_value_t val_type1 = esp_adc_cal_characterize(ADC_UNIT_2
88         , ADC_ATTEN_DB_11, ADC_WIDTH_12Bit, REF_VOLTAGE, adc_chars);
89
90     incomingChar = 'e';
91 }
92
93 // loop
94 void loop() {
95     handleSerial();
96     //float RTD_K = measure_RTD();
97     //Serial.println(RTD_K, 1);
98     if (measure){
99         unsigned long begin_time = micros();

```

```
95     uint16_t *array3 = read_sensor(array1);
96     unsigned long end_time = micros();
97     int sample_time = (end_time - begin_time) / size_of_data;
98     send_data(array3, sample_time);
99     measure = false;
100 }
101 }
```

```

1 #include "driver/adc.h"
2 #include "esp_adc_cal.h"
3 #include "SPIFFS.h"
4
5 const int data_length = 10000, multi_sample = 100;
6
7 // measurement loop initiation
8 bool measure = false;
9
10 // RTD_K coefficients
11 //const float RTD_a = 8.9494 * pow(10,-6);
12 //const float RTD_b = 0.2378;
13 //const float RTD_c = 26.25;
14 const float RTD_a = -5.3117*pow(10,-9);
15 const float RTD_b = 2.4274*pow(10,-5);
16 const float RTD_c = 0.2232;
17 const float RTD_d = -242.15;
18
19 // TC_K coefficients
20 const float TC_K_p1 = 3.2715 * pow(10,3);
21 const float TC_K_p2 = -1.4850 * pow(10,4);
22 const float TC_K_p3 = 2.6598 * pow(10,4);
23 const float TC_K_p4 = -2.3646 * pow(10,4);
24 const float TC_K_p5 = 1.0740 * pow(10,4);
25 const float TC_K_p6 = -1.8937 * pow(10,4);
26
27 const float R2 = 2140;
28 const float Vin = 3.3 ;
29 int SenVal[data_length], avg_sens[data_length/multi_sample], subset[
    multi_sample];
30 int val_sum = 0, val_average = 0;
31 unsigned long Time[data_length], avg_time[data_length/multi_sample];
32 unsigned long time_stamp;
33 String data_spacer_string = " ", RTD_K_string, TC_V_string,
    Full_file_name, Data_line, First_line;
34
35 String file_name = "data_file";
36
37 // define characterize ADC
38 #define REF_VOLTAGE 1114
39 esp_adc_cal_characteristics_t *adc_chars = new
    esp_adc_cal_characteristics_t;
40
41
42
43
44
45
46

```

```

47 // setup
48 void setup() {
49     // set baud speed
50     Serial.begin(115200);
51
52
53     // configure ADC2
54     adc2_config_channel_atten(ADC2_CHANNEL_3, ADC_ATTEN_DB_11); //GPIO
55     15 = ADC2_CH3
56     adc2_config_channel_atten(ADC2_CHANNEL_4, ADC_ATTEN_DB_11); //GPIO
57     13 = ADC2_CH4
58     adc2_config_channel_atten(ADC2_CHANNEL_5, ADC_ATTEN_DB_11); //GPIO
59     12 = ADC2_CH5
60     adc2_config_channel_atten(ADC2_CHANNEL_6, ADC_ATTEN_DB_11); //GPIO
61     14 = ADC2_CH6
62
63     // characterize ADC2
64     esp_adc_cal_value_t val_type1 = esp_adc_cal_characterize(ADC_UNIT_2
65         , ADC_ATTEN_DB_11, ADC_WIDTH_12Bit, REF_VOLTAGE, adc_chars);
66
67     // create file name
68     String Full_file_name = "/" + file_name + ".txt";
69
70     // list and delete all files
71     //create_file();
72     //Serial.println("\n\n---BEFORE REMOVING---");
73     //listAllFiles();
74     Delete_All_Files();
75     //Serial.println("\n\n---AFTER REMOVING---");
76     //listAllFiles();
77
78 }
79
80 // loop
81 void loop() {
82     handleSerial();
83
84     if (measure){
85         // Multisampling
86         float RTD_K_sum = 0;
87         float TC_V_sum = 0;
88         int sample_amount = 20;
89         for (int i = 0; i < sample_amount ; i++){
90             RTD_K_sum += Sence_temps_RTD_K();
91             TC_V_sum += Sence_vol_TC();
92         }
93         float RTD_K = RTD_K_sum / sample_amount;
94         float TC_V = TC_V_sum / sample_amount;
95         float TC_K = TC_vol_to_K(TC_V);

```

```

91
92 // print
93 Serial.print(RTD_K, 1);
94 Serial.print(" ");
95 Serial.println(TC_V, 1);
96
97 // write to file
98 Write_data(RTD_K, TC_V);
99
100 // delay
101 delay(1000);
102 }
103
104 }
105 }
106
107
108
109 // sence temp data from thermocouple
110 float Sence_vol_TC() {
111     int read_raw_TC;
112     adc2_get_raw( ADC2_CHANNEL_6, ADC_WIDTH_12Bit, &read_raw_TC); //
113     GPIO =
114     float TC_vol_mV = esp_adc_cal_raw_to_voltage(read_raw_TC,
115         adc_chars);
116     float TC_vol_V = TC_vol_mV * 0.001;
117     return TC_vol_mV;
118 }
119
120 // convert voltage TC to K
121 float TC_vol_to_K(float TC_vol){
122     float TC_K = TC_K_p1*pow(TC_vol,5)+TC_K_p2*pow(TC_vol,4)+TC_K_p3*
123         pow(TC_vol,4)+TC_K_p4*pow(TC_vol,2)+TC_K_p5*TC_vol+TC_K_p6;
124     return TC_K;
125 }
126
127 // sence temp data from RTD
128 float Sence_temps_RTD_K() {
129     int read_raw_RTD;
130     adc2_get_raw( ADC2_CHANNEL_3, ADC_WIDTH_12Bit, &read_raw_RTD);
131     float RTD_vol_mV = esp_adc_cal_raw_to_voltage(read_raw_RTD,
132         adc_chars);
133     float RTD_vol_V = RTD_vol_mV * 0.001;
134     float RTD_ohm = Vin*R2/(Vin-RTD_vol_V)- R2;
135     float RTD_K = RTD_a*pow(RTD_ohm,3) + RTD_b*pow(RTD_ohm,2) + RTD_c
136         *RTD_ohm + RTD_d;
137     //float RTD_K = RTD_a*sq(RTD_ohm) + RTD_b*RTD_ohm + RTD_c;
138     return RTD_K;
139 }
140

```

```

135 }
136 }
137
138 void Write_data(float RTD_K, float TC_V) {
139     Full_file_name = "/" + file_name + ".txt";
140     File fileToAppend = SPIFFS.open(Full_file_name, FILE_APPEND);
141     if (!fileToAppend){
142         Serial.println("There was an error opening the file for
143             appending");
144         return;
145     }
146     RTD_K_string = String(RTD_K,1);
147     TC_V_string = String(TC_V,4);
148     Data_line = RTD_K_string + "," + TC_V_string;
149     if (!fileToAppend.println(Data_line)){
150         Serial.println("File append failed");
151     }
152     fileToAppend.close();
153 }
154
155
156 void create_file(){
157     // setup file
158     Full_file_name = "/" + file_name + ".txt";
159     First_line = "RTD[K],TC[V]";
160     if (!SPIFFS.begin(true)) {
161         Serial.println("An Error has occurred while mounting SPIFFS");
162         return;
163     }
164     File fileToWrite = SPIFFS.open(Full_file_name, FILE_WRITE);
165     if (!fileToWrite){
166         Serial.println("There was an error opening the file for
167             writing");
168         return;
169     }
170     if (fileToWrite.println(First_line)){
171         //Serial.println("File was written");
172     } else {
173         Serial.println("File write failed");
174     }
175     fileToWrite.close();
176 }
177
178 void handleSerial() {
179     String Full_file_name = "/" + file_name + ".txt";
180     while (Serial.available() > 0) {
181         char incomingCharacter = Serial.read();

```

```

182     switch (incomingCharacter) {
183         case 'b':
184             //Serial.println("trying to create file");
185             create_file();
186             //Serial.println("file should be created");
187             measure = true;
188
189             break;
190         case 'e':
191             measure = false;
192
193             //Serial.println("Measuerement ended, start sending file");
194             send_file(Full_file_name);
195             //Serial.println("Finished sending file");
196             break;
197     }
198 }
199 }
200
201 void send_file(String Full_file_name) {
202     if(!SPIFFS.begin(true)){
203         Serial.println("An Error has occurred while mounting SPIFFS")
204         ;
205         return;
206     }
207     File file = SPIFFS.open(Full_file_name);
208     if(!file){
209         Serial.println("Failed to open file for reading");
210         return;
211     }
212     Serial.println("x");
213     while(file.available()){
214         Serial.write(file.read());
215     }
216     file.close();
217     Serial.println("y");
218 }
219 void listAllFiles(){
220     File root = SPIFFS.open("/");
221     File file = root.openNextFile();
222     while(file){
223         Serial.print("FILE: ");
224         Serial.println(file.name());
225         file = root.openNextFile();
226     }
227 }
228
229 void Delete_All_Files(){

```

```
230 File root = SPIFFS.open("/");
231 File file = root.openNextFile();
232 while(file){
233     SPIFFS.remove(file.name());
234     file = root.openNextFile();
235 }
236 }
```

Bibliography

- [1] M. C. Scott, Chien Chun Chen, Matthew Mecklenburg, Chun Zhu, Rui Xu, Peter Ercius, Ulrich Dahmen, B. C. Regan, and Jianwei Miao. Electron tomography at 2.4-ångström resolution. *Nature*, 483(7390):444–447, 2012.
- [2] J. Dubochet and A. W. McDowell. Vitrification of Pure Water for Electron Microscopy. *Journal of Microscopy*, 124(3):3–4, 1981.
- [3] L. A. Passmore and C. J. Russo. *Specimen Preparation for High-Resolution Cryo-EM*, volume 579. Elsevier Inc., 1 edition, 2016.
- [4] Miroslava Schaffer, Benjamin D Engel, Tim Laugks, Julia Mahamid, and Jürgen M Plitzko. Cryo-focused Ion Beam Sample Preparation for Imaging Vitreous Cells by Cryo- electron Tomography. *Bio-protocol*, 5(17), 2015.
- [5] Hans Moor. Cryotechnology for the structural analysis of biological material. In *Freeze-Etching: Techniques and applications*, pages 11 – 20. 1973.
- [6] W. B. Bald. *Quantitative cryofixation*. CRC Press, 1st edition, 1987.
- [7] Keith Patrick Ryan. *Rapid Cryogenic Fixation of Biological Specimens*. PhD thesis, Plymouth University, 1991.
- [8] W. B. Bald. On crystal size and cooling rate. *Journal of Microscopy*, 143(1):89 – 102, 1986.
- [9] Corinne Blancard and Bénédicte Salin. Plunge freezing: A tool for the ultrastructural and immunolocalization studies of suspension cells in transmission electron microscopy. *Journal of Visualized Experiments*, 2017(123):1–9, 2017.
- [10] Krzysztof Bobik, John R. Dunlap, and Tessa M. Burch-Smith. Tandem high-pressure freezing and quick freeze substitution of plant tissues for transmission electron microscopy. *Journal of Visualized Experiments*, (92):1–10, 2014.
- [11] CryoSol. Vitrojet. <https://www.cryosol-world.com/vitrojet/>.
- [12] DELMIC. Survey among customers on sample preparation. Technical report, 2018.
- [13] B. Luyet and F. Gonzales. Recording Ultra Rapid Changes In Temperature. *Refrigerating Engineering*, pages 1191 – 1193, 1236, 1951.
- [14] Hye-Jin Cho, Jae-Kyung Hyun, Jin-Gyu Kim, Hyeong Seop Jeong, Hyo Nam Park, Dong-Ju You, and Hyun Suk Jung. Measurement of ice thickness on vitreous ice embedded cryo-EM grids: investigation of optimizing condition for visualizing macromolecules. *Journal of Analytical Science and Technology*, 4(1):7, 2013.

- [15] William F. Tivol, Ariane Briegel, and Grant J. Jensen. An Improved Cryogen for Plunge Freezing William. *Microsc Microanal*, 14(5):375–379, 2008.
- [16] Keith P Ryan. Cryofixation of tissues for electron microscopy: a review of plunge cooling methods, 1992.
- [17] W. B. Bald. The relative efficiency of cryogenic fluids used in the rapid quench cooling of biological samples. *Journal of Microscopy*, 134(3):261–270, 1984.
- [18] S. G. Ryan, D. H. Purse, S. G. Rostnson, and J. W. Wood. The relative efficiency of cryogenes used for plunge-cooling biological specimens. *Journal of Microscopy*, 145(1):89–96, 1987.
- [19] K P Ryan, W B Bald, D H Purse, D N Nicholson, Citadel Hill, Universitiit Saarlandes, and Universitiit Salzburg. Cooling rate and ice-crystal measurement in biological specimens plunged into liquid ethane, propane, and Freon 22. *Journal of Microscopy*, 158(3):365–378, 1990.
- [20] M.J. Costello, R. Fetter, and J.M Corless. Optimum conditions for the plunge freezing of sandwiched samples. *The Science of Biological Specimen Preparation*, pages 105–115, 1984.
- [21] M.J. Costello. The direct measurement of temperature changes within freeze-fracture specimens during rapid quenching in liquid cool.pdf. *Journal of Microscopy*, 112(1):17–37, 1978.
- [22] Keith Patrick Ryan and David H. Purse. Rapid freezing- specimen suport and cold gass layers.pdf. *Journal of Microscopy*, 163(3):RP5–RP6, 1984.
- [23] Stuart M. Bailey and Joseph A. N. Zasadzinski. Validation of convection-limited cooling of samples for freeze-fracture electron microscopy. *Journal of Microscopy*, 163(3):307–320, 1991.
- [24] Joseph A. Zasadzinski. A new heat transfer model to predict cooling rates for rapid freezing fixation. *Journal of Microscopy*, 150(2):137 – 149, 1988.
- [25] S. Kasas, G. Dumas, G. Dietler, S. Catsicas, and Marc Adrian. Vitrification of cryoelectron microscopy specimens revealed by high-speed photographic imaging. *Journal of Microscopy*, 211(1):48–53, 2003.
- [26] A.F. Mills. *Basic Heat and Mass Transfer*. Pearson Education (Us), second edition, 1998.
- [27] G. H. Gelb, B. D. Marcus, and D. Dropkin. Manufacture of fine wire thermocouple probes. *Review of Scientific Instruments*, 35(1):80–81, 1964.
- [28] Demetre E Tsatis. Thermal diffusivity of GE-7031 varnish. *Journal of Applied Physics*, 62(1):302, 1987.
- [29] N. J. Simon and E. S. Drexler. Properties of Copper and Copper Alloys at Cryogenic Temperatures. *National Institute of Standards and Technology (NIST)*, page 270, 1992.
- [30] Mathworks. MATLAB - smoothdata. <https://www.mathworks.com/help/matlab/ref/smoothdata.html> 'rloess'—.
- [31] REOTEMP Instruments. Type-K Thermocouple Reference Table. <https://www.thermocoupleinfo.com/type-k-thermocouple.htm>.

- [32] W. B. Bald. The relative merits of various cooling methods.pdf. *Journal of Microscopy*, 140(1):17–40, 1985.
- [33] N. R. Silvester, S. Marchese-Ragona, and D. N. Johnston. The relative efficiency of various fluids in the rapid freezing of protozoa. *Journal of Microscopy*, 128(2):175–186, 1982.